Image Cover Sheet

CLASSIFICATION	SYSTEM NUMBER
UNCLASSIFIED	500782

TITLE

DEVELOPMENT OF A TIME-INTEGRATING CORRELATOR FOR THE PROCESSING OF SPREAD SPECTRUM SIGNALS

System Number:

Patron Number:

Requester:

Notes:

DSIS Use only:

Deliver to:

National Defence / Défense nationale

DEVELOPMENT OF A TIME-INTEGRATING CORRELATOR FOR THE PROCESSING OF SPREAD SPECTRUM SIGNALS (U)

by

N. Brousseau and J.W.A. Salt

DEFENCE RESEARCH ESTABLISHMENT OTTAWA
REPORT NO. 1298

Canada

November 1996
Ottawa

National Defence / Défense nationale

DEVELOPMENT OF A TIME-INTEGRATING CORRELATOR FOR THE PROCESSING OF SPREAD SPECTRUM SIGNALS (U)

by

N. Brousseau and J.W.A. Salt
Electronic Support Measures Section

DEFENCE RESEARCH ESTABLISHMENT OTTAWA
REPORT NO. 1298

PROJECT
5BB16

November 1996
Ottawa

ABSTRACT

An optoelectronic processor was built at DREO for the detection and processing, of spread spectrum radar and communication signals in presence of noise and interfering signals. The design and performance of the processor, a Time-Integrating Correlator (TIC), are presented. A general description of the TIC, of its operation, components and subsystems is included. The signal processing and the data collection procedure are also described. The digital controller, the packaging of the system and the effects of the temperature changes on the stability of the TIC are presented.

Experimental measurements of the performance of the TIC were performed with binary phase shift keyed input signals with chip rates up to 20 MHz and the results are included. The TIC has a 30 MHz bandwidth and can detect reliably correlation peaks on a time difference of arrival window of 90 μs. The dynamic range of the prototype is 60 dB and it can produce detectable correlation peaks in additive white Gaussian noise for input signals having a signal to noise ratio of -35 dB while using a processing gain of 40 dB. The performance of the TIC, for that particular set of parameters, is thus within 5 dB from the theoretical limit.

RESUME

Un système optoélectronique fut construit au CRDO pour la détection et le traitement, de signaux à spectre étalé de radar et de communication en présence de bruit et d'interférences. On présente la conception et les performances du corrélateur à integration temporelle (CIT) ainsi que sa description générale, son mode d'opération, ses composantes et sous- systèmes. Les techniques de traitement des signaux et d'acquisition des données, le contrôleur numérique, le montage, et les effets des changements de température sont aussi décrits.

Des mesures expérimentales furent effectuées en utilisant des signaux à modulation par déplacement binaire de phase dont le taux variait jusqu' à 20 MHZ. Le CIT a une bande passante de 30 MHZ et il peut détecter de façon fiable des corrélations sur une fenêtre de 90 μs. La plage dynamique du prototype est de 60 dB et il peut produire, avec un gain de 40 dB, des corrélations détectables avec un rapport signal sur bruit du signal d'entrée de -35 dB dans du bruit blanc gaussien additif. Ce résultat se situe à 5 dB de la limite théorique.

EXECUTIVE SUMMARY

An optoelectronic processor was built at DREO for the detection and processing, of spread spectrum radar and communications signals in presence of noise and interfering signals. This processor, a Time-Integrating Correlator (TIC), is an analog optical computer designed to correlate two large bandwidth data streams of long duration. TICs can be used to compare signals in civilian applications such as DNA analysis and search of large unstructured data base of various kind.

Military applications of TICs are related to the processing of large bandwidth radar and communication spread spectrum signals for Electronic Intelligence (ELINT) and Electronic Support Measures (ESM). TICs can be applied to the real-time, large bandwidth implementation of new advanced signal processing algorithms such as the cyclic crosscorrelation. This algorithm has the capability to separate spread spectrum signals sharing the same bandwidth, the same carrier frequency and the same time difference of arrival at negative signal to noise ratios. Because of these attributes, the cyclic crosscorrelation implemented with a TIC has a great potential for the development of ELINT and ESM receivers for low probability of intercept radar and communication spread spectrum radar.

This report describes the design and performance of a TIC built at DREO for the processing of spread spectrum signals. A General Description of the TIC, of its operation, components and subsystems is presented. The signal processing and the data collection procedure are also described. The digital controller, the packaging of the system and the effects of the temperature changes on the stability of the TIC are summarized.

Experimental measurements of the performance of the TIC are included. The TIC has a 30 MHz bandwidth and can detect reliably correlation peaks on a time difference of arrival window of 90 μs. The dynamic range of the prototype is 60 dB and it can produce detectable correlation peaks in additive white Gaussian noise for input signals having a signal to noise ration of -35 dB while using a processing gain of 40 dB. The performances of the TIC are thus within 5 dB from the theoretical limit. The inputs to the TIC were binary phase shift keyed signals with Chip rates up to 20 MHz.

TABLE OF CONTENTS

TABLE OF CONTENTS

LIST OF FIGURES

LIST OF TABLES

LIST OF ABBREVIATIONS

DARPA:	Defence Advanced Research Development Agency
DC:	Digital Controller
DREO:	Defence Research Establishment Ottawa
ELINT:	Electronic INTelligence
ESM:	Electronic Support Measures
MICOM:	Missile Command
RF:	Radio Frequency
SNR:	Signal to Noise Ratio
TIC:	Time-Integrating Correlator
TOPS:	Transition of Optical Processors into Systems
US:	United States

1.0 INTRODUCTION

An optoelectronic processor was built at the Defence Research Establishment Ottawa (DREO) for the detection and processing, of spread spectrum radar and communication signals in presence of noise and interfering signals. The processor, a Time-Integrating Correlator (TIC), is an analog optical computer designed to correlate two large bandwidth data streams of long duration. The two Radio Frequency (RF) input waveforms are introduced in the optical system via acousto-optic interaction in Bragg cells. The correlation of the waveforms is produced when the images of the two light distributions generated by the data streams in the Bragg cells are coherently added and time-integrated by a detector array.

1.1 Potential Applications of TICs

Two military applications of the real-time processing of spread spectrum signals have been demonstrated at DREO with a 30 MHz bandwidth TIC. In the first experiments, a TIC was used to perform signal compression for low probability of intercept signals using a BPSK modulation [1]. In the second experiment, a TIC was used for the real-time implementation of the cyclic crosscorrrelation [2]. This algorithm has the capability to separate spread spectrum signals sharing the same bandwidth, the same carrier frequency and the same difference of time of arrival at negative signal to noise ratios. Because of these attributes, the cyclic crosscorrelation has great potential for the development of ELINT and ESM receivers for spread spectrum signals.

Searches of large unstructured data bases of various kind are also an interesting field of applications for TICs. A proof-of-concept experiment was performed at DREO [3-4] to demonstrate the potential of TIC to perform very fast human DNA analysis. The decision on the identity or similarity of the signals representing DNA sequences was based on the amplitude of the correlation peaks produced by the TICs.

Other important military applications of TICs are related to the processing of large bandwidth radar and communication spread spectrum signals for Electronic Intelligence (ELINT) and Electronic Support Measures (ESM) [5]. The development of some TIC based military processors is stimulated by the Transition of Optical Processors into Systems (TOPS) program sponsored by the Defence Advanced Research Project Agency (DARPA) [6]. Among the processors that are developed by the TOPS program are wideband processors for carrier frequency and envelope modulation analysis [7]. Other processors are designed to implement adaptive jamming [8]. Also under development is a system to perform range and Doppler processing on the spread spectrum MICOM radar of the US [9].

1.2 Content of the Report

This report describes the design and performances of a TIC built at DREO for the detection and processing of spread spectrum signals. It is the system that was used for the DREO proof-of-concept experiments mentioned in Section 1.1. Section 2 contains a general description of the TIC and of its operation. Sections 3 to 6 contain a description of the sub-systems and components developed to build the TIC. Sections 7 and 8 respectively describe the signal processing associated with the pedestal removal and the data collection with the detector array. Section 9 analyses the effects of temperature changes on the stability of the TIC and Section 10 describes the mounting and packaging of the system. The TIC is an optoelectronic hybrid system requiring an optical correlator and a Digital Controller (DC). Section 11 describes the DC associated with the TIC. The performances of the system are presented in Section 12. The testing of the TIC was performed with Binary Shift Keyed (BPSK) signals with a chip rate of up to 20 MHz. Experimental measurements have demonstrated the capability of the TIC to detect reliably correlation peaks for a Time Difference of Arrival (TDOA) window of 90 μs. The dynamic range of the prototype is 60 dB. It can produce detectable correlation peaks, while using a processing gain of 40 dB, when additive white Gaussian noise is added to one of the input signals giving a signal to noise ration of -35 dB. This result is within 5 dB from the theoretical limit. Section 13 presents the conclusion and suggestion for future work.

2.0 DESCRIPTION OF THE DREO TIME-INTEGRATING CORRELATOR

The first operation performed by a TIC is the transformation of the RF signals a(t) and b(t) to be correlated, into light modulated beams (Figure 1). Each RF signals is applied to a light modulator called Bragg cell. A Bragg cell consists of a piezoelectric transducer attached to a crystal in which acoustic waves are generated. When a RF signal is applied to the transducer, acoustic waves are generated and propagate in the Bragg cell crystal. A moving grating of changing indices of refraction is thus formed. The gratings in the Bragg cells are illuminated by two expanded laser beams originating from the same laser and each beam interacts with the acoustic waves of only one Bragg cell. Some of the incident light is diffracted by the gratings and therefore, the information contained in the RF signals is simultaneously transferred to the diffracted laser beams. The system is layed out in such a way that the signals propagate in opposite direction in each Bragg cell, a condition needed for the correlation. The gratings are then imaged, with lenses, onto a detector array where they remain counter propagating. The 5000-element detector array performs a time integration of the coherent addition of the two images of the signals.

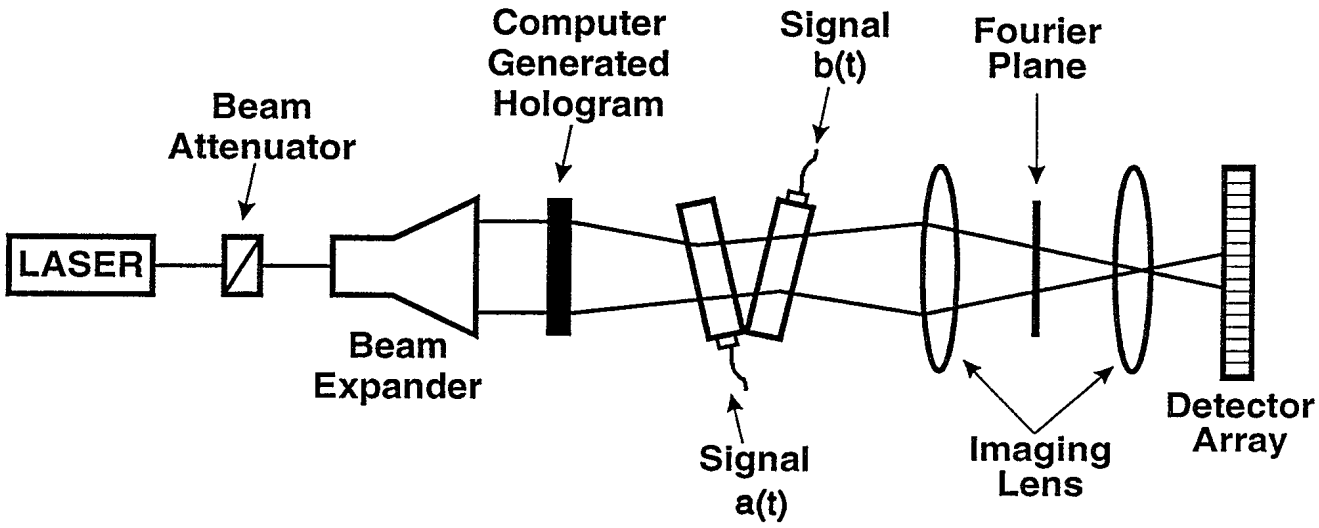

FIGURE 1: SCHEMATIC OF THE TIME-INTEGRATING CORRELATOR.

If the variable z is the distance along the Bragg cells and if the origin z=0 is defined to be at the center of the Bragg cells and, correspondingly at the centre of their images on the detector array, the optical signals diffracted by the Bragg cells are a(t+z/v) and b(t-z/v), where v is the velocity of propagation of the signals in the Bragg cells. The electrical signal produced by the detector array, s(t,z), is proportional to the square of the light distribution.

$$s(t,z) = | a(t+z/v) + b(t-z/v) |^2 \quad (1)$$

$$= a^2(t+z/v) + b^2(t-z/v) + 2\, a(t+z/v)\, b^*(t-z/v) \quad (2)$$

This response is then integrated for a duration T and the resulting signal S(T,z) is

$$s(T,z) = \int_0^T [\, a^2(t+z/v) + b^2(t-z/v) + a(t+z/v)\, b^*(t-z/v)\,]dt \quad (3)$$

The response of all the individual elements of the detector array is called a correlogram (Figure 2). The third term of Equation 3 is the correlation of the input data a(t) and b(t). This correlation term is observed as a peak on a pedestal generated by the first and second term of the equation. The presence of the peak indicates that the two input signals a(t) and b(t) are identical conversely, the absence of the correlation peak indicates that the two inputs are different. However, the presence of a correlation peak with a reduced amplitude can indicate a partial match between the signals [3-4]. Figure 2a illustrates a pedestal and a correlation peak where the Gaussian shape of the pedestal is noticeable. It is an expanded version of the Gaussian profile of the illuminating laser beam. Figure 2b illustrates a modulated correlation peak. The modulation is produced by the selection of the operating parameters for the TIC and can be adjusted at will. This feature is discussed in Section 8 on optimal data collection.

A photograph of a TIC is presented in Figure 3. Some of the advantages of this implementation are a relatively low volume that can be packaged into 10 inch high of a 19 inch rack. The power consumption is less than 500 watts. The Bragg cells have a 30 MHz bandwidth centered at 45 MHz and make this TIC well suited for the processing of spread spectrum communication or radar signals. The detector array has 5000 elements and the minimum real-out time of the array is 200 μs. The correlation is formed by the detector array through an integration of duration T. At the end of the integration time T, the correlation is already fully formed by the detector array and is clocked out. The illumination is provided by a 20 mw helium-neon laser operating on the red line at 632.8 nm.

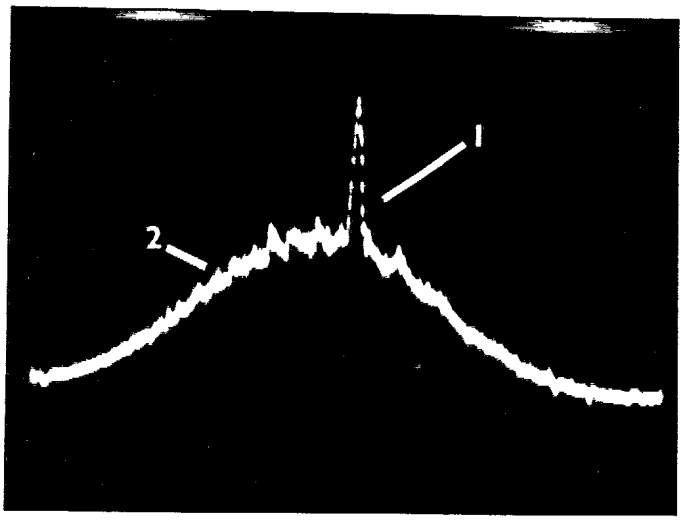

A) UNMODULATED PEAK

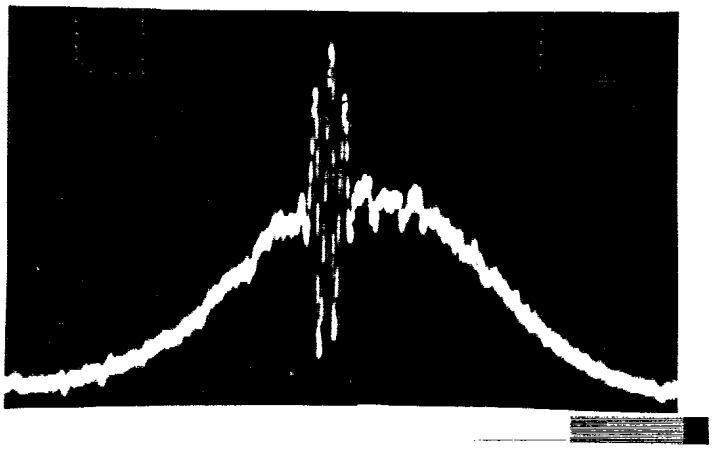

B) MODULATED PEAK.

FIGURE 2: CORRELATION PEAK ON A GAUSSIAN PEDESTAL

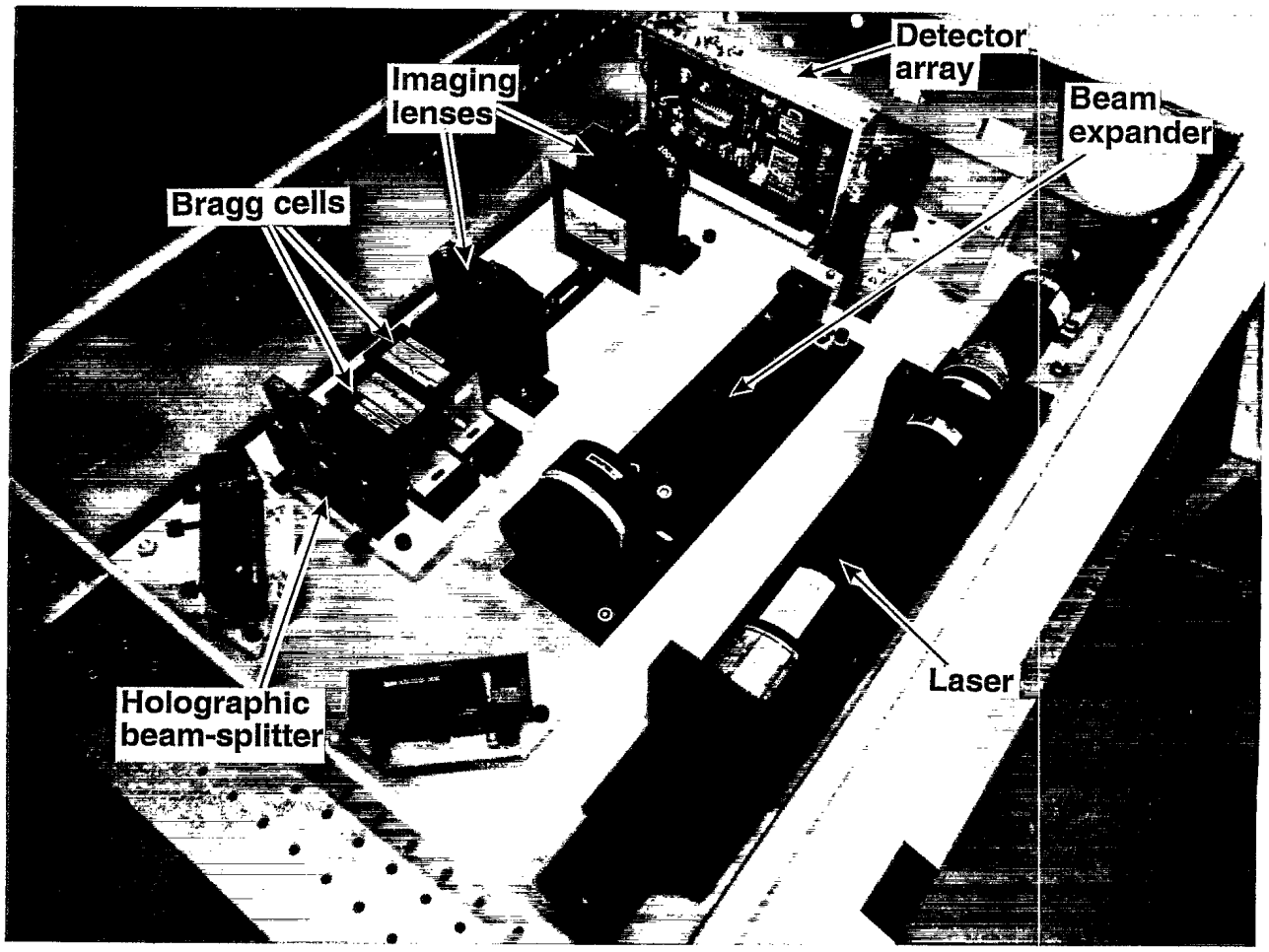

FIGURE 3: PHOTOGRAPH OF A TIC MOUNTED IN A 19-INCH RACK.

The TIC is a hybrid optoelectronic system including a 486 personal computer whose main functions are to send the input signal to the Bragg cells, control the read-out of the detector array and perform the removal of the pedestal to facilitate the detection of the peak. The DC also contains statistical algorithms to further analyse the result from the TIC. Various techniques have been proposed and assessed at DREO [10] to perform pedestal removal and a summary of the results can be found in Section 7.0.

3.0 ILLUMINATION FOR TIME-INTEGRATING CORRELATORS

One of the most critical requirements for a TIC is the capability to produce correlation peaks of uniform height over the whole width of its aperture. This requirement generates important demands on the illumination system. Another desirable feature of the DREO TIC is the capability to operate with integration times that vary between 250 μs and 50 ms. In order to avoid the saturation of the detector array, the illumination has to be adjusted as a function of the integration time.

The control of the phase error at the output of the TIC is also an important issue. Phase error has multiple origins such as imperfect optical components, misalignment of otherwise perfect components, temperature changes [11] and atmospheric turbulence. The effect of phase error have been described in detail [12] and a data collection method that tolerates a moderate amount of phase error has been proposed at DREO[12]. Nevertheless, phase errors still have to be controlled and optical components of a sufficient quality have to be used in the illumination system as in the other parts of the system, although diffraction limited performance is not required.

3.1 Design of the Illumination System

The illumination system selected for the TIC includes a He-Ne laser producing a .68 mm diameter pencil beam with a Gaussian intensity profile that passes through an attenuator. The attenuator consists of a polarizing cube beam splitter that is rotated to change the attenuation of the light. The Gaussian laser beam is then expanded by an anamorphic beam-expander into a line of light with a uniform intensity. The line of light is finally separated into two identical beams propagating at an angle of 4.06 degrees. Each of these two beams interacts with only one of the Bragg cells. The following sections contain details about the design, construction and performance of these components of the illumination system.

3.2 Selection of the Laser

A few important factors must be taken into account when selecting the source of laser light for a TIC. Some of these requirements are conflicting. Therefore, compromises must be made. For example, a very small laser is easier to package, however, the laser must produce enough power to operate the system, and small

lasers produce small power output. Another selection criterion is the stability of the mode of the output of the laser. The laser must operate in the fundamental mode, which is characterized by a Gaussian distribution of the output light. Other transversal modes which produce light distributions having bright and dark spots are unacceptable. The amount of heat dissipated by the laser is also a concern because it could affect the thermal stability of the whole TIC package and may even lead to cooling requirements.

The laser must also operate at a wavelength for which a sensitive linear detector array is available to detect the light distributions produced by the TIC. This limits the range of wavelengths to the visible or the near infrared. The red end of the spectra is preferred because the PIN photodiodes that are used as detectors are most sensitive to red light. Reliability is also important.

The two obvious choices meeting the above criteria are HeNe lasers or laser diodes. Laser diodes operating at 850 nm were seriously considered, but they were rejected because of the cost and of the unacceptable delays that were associated with the conversion of the laboratory operation from HeNe to near infrared. The cost and delays were caused mainly by the need to replace the anti-reflection coating of all the optical equipment and by the procurement of new Bragg cells optimized for operating at 850 nm. While this work was done, visible laser diodes operating around 630 nm with sufficient power and stability were under development, but not yet available. So a 20 mw HeNe laser operating at 633 nm was selected because it provide the fundamental mode operation, and the power required at an acceptable wavelength.

3.3 Attenuation of the Light

The TIC is expected to operate with integration time varying between 250 μs and 50 ms and the light attenuator has to provide the capability to adjust the illumination level from 50% to 85% of the saturation level of the detector for this range of integration times. The attenuator selected for the DREO TIC consists of a polarizing beam-splitter cube set on a rotation stage. A 45° rotation of the cube changes the intensity of the transmitted beam from 0.4% to 99.0% of the incident beam as illustrated in Figure 4. As the cube rotates, the polarization of the transmitted beams also rotates. The resulting polarization changes of the transmitted beam does not affect the performance of the TIC because of the small angle between the beams interfering on the detector array. The range of attenuation provided by the attenuator is sufficient to allow the operation within the range of specified integration times.

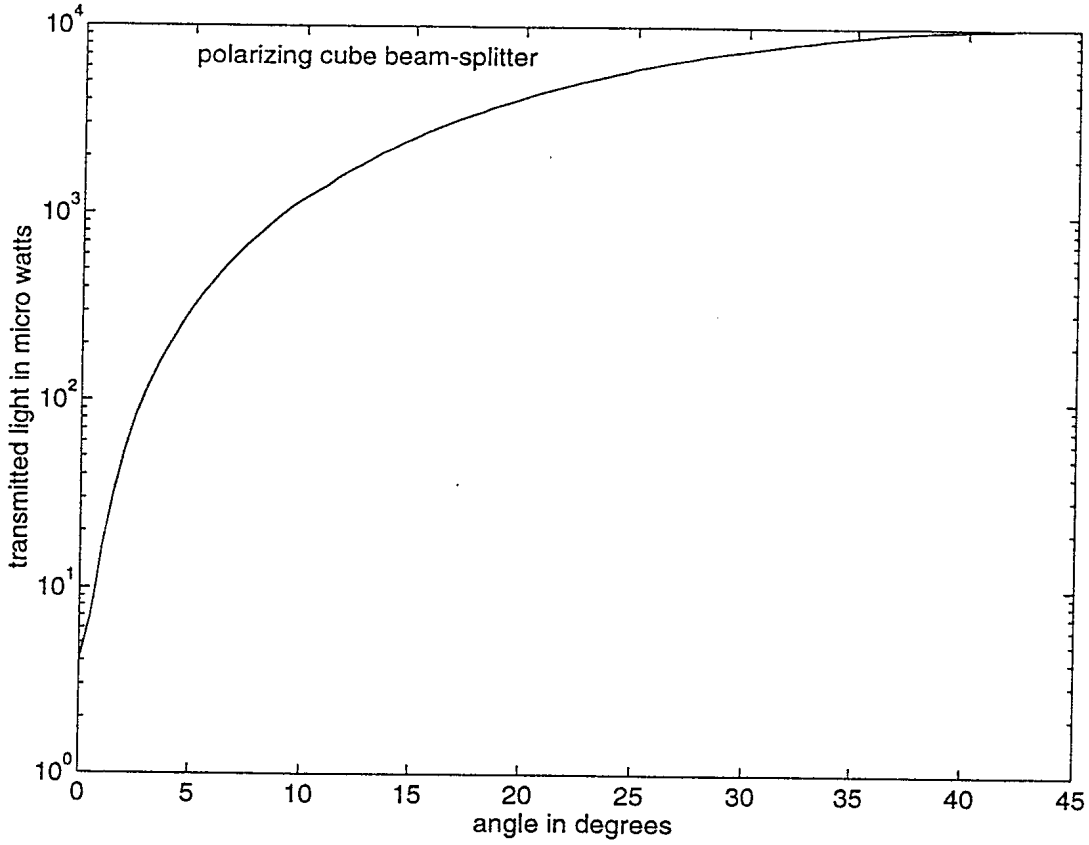

FIGURE 4: LIGHT TRANSMITTED BY THE POLARIZING BEAM SPLITTER.

3.4 Beam-Expansion

The purpose of the beam-expander is to produce a uniform illumination of the Bragg cells with minimum phase error and minimum loss of light. The requirement for a uniform illumination originates from equation 3. Inspection of equation 3 shows that the height of the peak above the pedestal cannot exceed the height of the pedestal. As the maximum height of the peak above the pedestal is set by the height of the pedestal, the pedestal has to have a uniform amplitude over the width of the TIC aperture to ensure the formation of a peak with uniform height over the whole aperture of the TIC. The requirement to achieve a low loss beam expansion is met by matching the dimensions of the illumination pattern to the dimensions of the active area (1 mm x 35 mm) of the Bragg cells. Minimum phase error is achieved by selecting good quality optical components.

3.4.1 Description

The beam-expander designed and constructed at DREO is illustrated in Figure 5. The Gaussian beam from the laser is expanded, on the horizontal axis, into a diverging line of light by a special anamorphic lens. The diverging line beam is then collimated by a spherical lens of proper focal length. Expansion of the beam with cylindrical lenses only was rejected because the expanded beam still retains its original Gaussian profile.

3.4.2 The Powell Lens

The anamorphic lens used to perform the beam expansion was designed at NRC by Dr. I. Powell [13] for the purpose of transforming a parallel laser beam with a Gaussian intensity distribution into a diverging uniform line of light. The Powell lens has to be matched to the diameter and divergence of the Gaussian beam to be expanded. They are available at low cost ($100) in a selection of diverging angles. The Powell lens has power only on one axis and leave the light distribution from the laser unchanged on the other axis.

3.4.3 The Collimating Lens

The purpose of the collimating lens is to transform the diverging line of light produced by the Powell lens into a parallel one. The focal length of the collimating lens and the divergence of the Powell lens were chosen to produce a line of light of the desired length. It is also required to keep the length of the beam expander to a minimum to facility the construction of a compact TIC. A spherical lens, with a focal length of 250 mm, designed to collimate a spherical beam, was selected rather than a cylindrical lens of the same quality and focal length because of its lower cost. They both achieved the same results on the horizontal axis. However, the spherical lens adds some focal power to the vertical axis of the light distribution but it is not detrimental to the operation of the TIC.

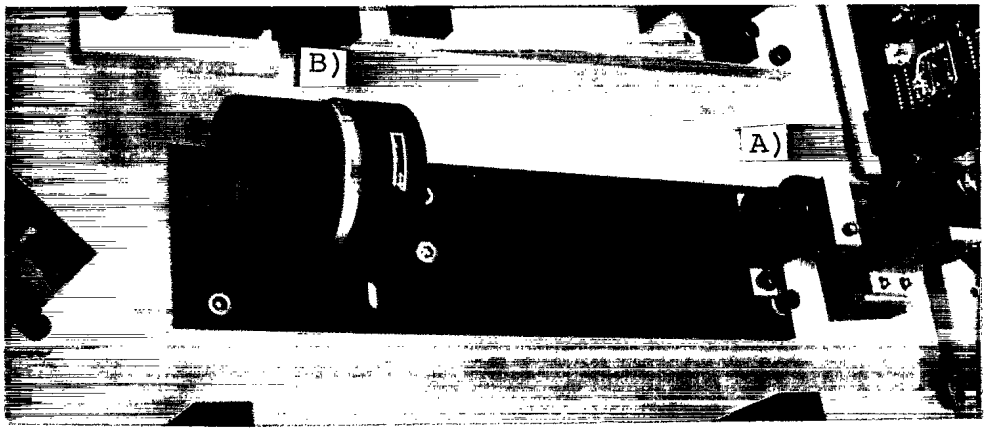

FIGURE 5: BEAM-EXPANDER.
A) POWELL LENS
B) COLLIMATING LENS

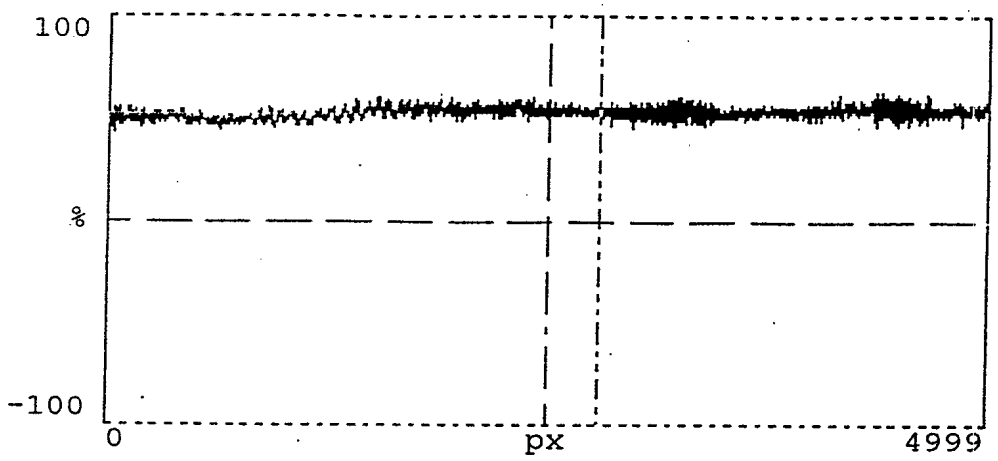

FIGURE 6: UNIFORM, EXPANDED ILLUMINATION .

3.4.4 Performances

The uniformity of the light distribution and the quality of the phase distribution produced by the beam expander were measured. Figure 6 illustrates the light distribution produced by the beam expander as detected by a 5000-element detector array. The horizontal axis is labelled in term of the elements of the detector array called pixels. Each pixel is 7 μm x 7 μm. The middle section (1 mm by 35 mm) of the line of light produced by the beam expander contains 80% of the light.

The phase error was evaluated using a beam-shearing interferometer and the resulting interferogram is illustrated on Figure 7 (actual size). One can see that there is little phase error on the horizontal axis because the fringes are almost horizontal. The phase distribution exhibit some error at both ends; as can be seen by the fringes curving upward at the right and downward at the left, but the middle 30 mm is almost perfect. The fringe pattern on the vertical axis is caused by the focal power introduced on that axis by the spherical collimating lens of the beam expander.

These results compare very favourably with the expansion of a Gaussian beam performed by a commercial beam expander made of spherical lenses. In that case the expanded beam still has a Gaussian profile and only a small part of the middle section can be used if a uniform (within certain criteria) beam is desired. The performance of such system was measured for comparison purposes. The laser beam was expanded into a 50 mm diameter circular beam. An aperture of 1 mm x 35 mm located in the middle of the expanded beam was transmitting only 1% of the laser power. The intensity variations from the edge to the middle 35 mm segment of the beam was 18%.

3.5 The Beam-Splitter

The function of the beam-splitter is to separate the line of light produced by the beam expander into two beams propagating at 4.06° from each other. This angle was calculated to produce the fringe system required for the optimal detection techniques described in [12]. Each of the two beams interacts with only one of the Bragg cells. Ideally, the beam-splitter should produce only the two desired beams, each containing 50% of the incident light.

3.5.1 Description

The beam-splitter used in the DREO TIC is a Dammann grating designed and constructed with diffractive optics technology (14). The particular Dammann grating considered here is computer generated with a periodic binary phase modulation implemented in a photo resistor layer. It is optimized for the wavelength of the HeNe laser, 633 nm. The grating size is 35 mm x 35 mm.

FIGURE 7: PHASE ERROR OF THE ILLUMINATION.

3.5.2 Efficiency

The diffraction efficiency in the various orders of the beam-splitter was measured. The results are presented in Table 1. One notices that 5% of the light is reflected and that 43.9% and 43.4% of the diffracted light is in the order +1 and -1 that are used to illuminate the Bragg cells. 0.17% of the transmitted light is undiffracted and has to be removed by filtering in the Fourier plane by a small wire of appropriate size. The diffraction efficiency was measured at many points on the 35 mm by 35 mm Dammann grating and was found to be uniform to within 1% which was the precision of the measuring equipment.

TABLE 1: INTENSITY OF THE DIFFRACTION ORDERS OF THE DAMMANN GRATING BEAM SPLITTER

DIFFRACTION ORDER	DIFFRACTION EFFICIENCY %
+4	0.18%
+3	4.6%
+2	0.1%
+1	43.9%
0	0.17%
-1	43.4%
-2	0.1%
-3	4.6%
-4	0.1%
reflected light	5.0%

3.5.3 Phase Error

The quality of the phase distribution produced by the Dammann grating beam-splitter was evaluated with a beam shearing interferometer. The interferogram of the incident illumination is shown as a reference in Figure 8a (actual size). The beam shearing interferograms of the +1 and -1 order are illustrated in Figure 8b (actual size) and 8c (actual size) respectively. It is possible to interpret these interferograms by remembering that a perfect, aberration free wavefront would give perfectly parallel and straight fringes. The distance between two fringes correspond to one wavelength. The slight curvature observed in the three interferograms indicate the presence of a very small amount of aberration. It can also be noted that the Dammann grating add very little aberration to the whole illuminating beam. The aberration added by the Dammann on a rectangle of the size of the aperture of the Bragg cells (1 mm x 30 mm) is negligible.

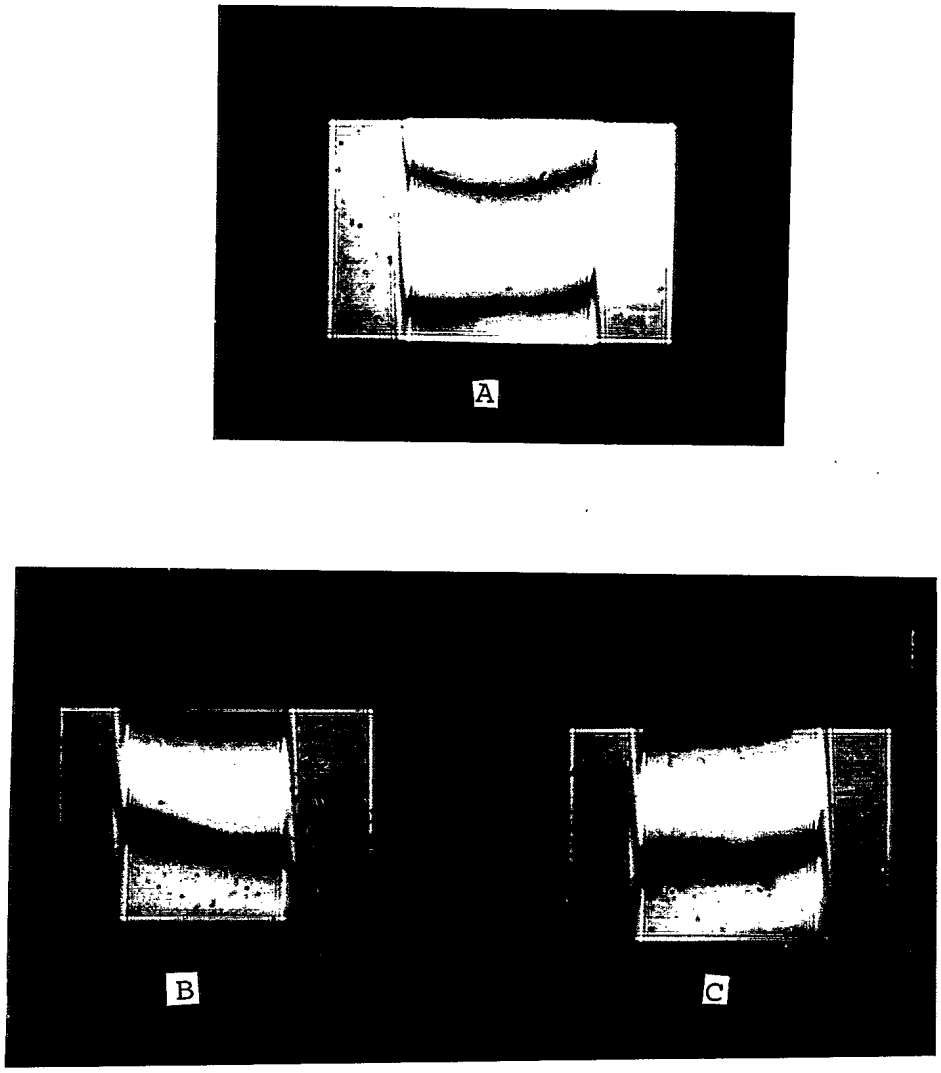

FIGURE 8: PHASE ERROR OF THE BEAM SPLITTER.

3.6 Performances

The efficiency of the illumination system of a TIC is defined as the percentage of light emitted by the laser that reaches the Bragg cells at the Bragg angle. In the case considered here the efficiency of the illumination system is the product of the efficiency of the three sub-systems used to build the illumination system. The attenuator, at maximum transmission, transmits 99% of the light it receives. The beam-expander produces a line of light that contents 80% of the incident light and the Dammann grating beam splitter diffracts 87% of the incident light into the +1 and -1 order illuminating the Bragg cells. The efficiency of the illumination system is thus 69%. Such good efficiency allows to use a smaller laser that is easier to package and that generates less heat to dissipate.

4.0 THE BRAGG CELLS

The key components of a TIC are the Bragg cells: they are used to convert the RF signals to modulate the laser light for eventual correlation. Bragg cells are made of a piezoelectric transducer attached to a transparent crystal. The input RF signals are applied to piezoelectric transducers attached to the Bragg cell crystal and acoustic are generated. The acoustic wave propagates through the Bragg cells at a velocity v and it takes a time τ for the waves to travel through the Bragg cells. τ is called the time-aperture of the Bragg cells. The signal propagating in the Bragg cells have to be imaged with lenses on the detector array. This task is made easier if the Bragg cells are short. Therefore, optical material with a slow acoustic velocity of propagation (v) are used to obtain large time-aperture and short physical length for the Bragg cells. Low attenuation of the acoustic waves is also required to maintain a signal level that is sufficient for the diffraction of the laser light. Large time-aperture devices have acousto optic crystal usually made of tellurium dioxide (TeO2) that operate in the slow-shear mode. In this case the velocity of acoustic waves in TeO2 is 617 m/s. Hence, a device with a 100 μs interaction time is 62 mm long. Devices with time-apertures as large as 100 μs are available commercially. The dynamic range, polarization and frequency response of Bragg cells have been extensively studied and are well documented [15-18]. A 50 μs window (31 mm) aperture was selected for the prototype to allow the implementation of the imaging system with relatively inexpensive commercially available lenses.

5.0 THE IMAGING SYSTEM

The light diffracted by the Bragg cells was imaged on the detector array by two Cooke triplets with a focal length of 100 mm and an entrance pupil of 35.7 mm set back-to-back. The two lenses operate close to optimal conditions: the parallel light that enters the first lens is focussed in the Fourier plan where filtering of

high diffraction orders take place. The light then diverges and is focussed onto the detector array by the second lens. This compact configuration was adjusted to produce a magnification of 1.17. Because the Fourier plane is easily accessible, it can be used to perform bandpass filtering, remove the undiffracted light, or possibly, perform interference excision.

6.0 THE DETECTOR ARRAY

A 5000-element Kodak detector array was selected for the TIC. The element are 7 μm x 7 μm. The odd and even elements of the detector array are clocked out by two separate shift registers operating at a clock rate up to 10 MHz. The combination of the output of the two shift registers produces a resulting clock out rate up to 20 MHz and the minimum integration time associated with the maximum clock rate is 250 μs. In practice, it was not possible to use a read-out rate of more than 6.6 MHz and the integration time had to be less than 820 μs in order to avoid producing severe distortion of the output signal. The dynamic range of the detector array was specified by the manufacturer as 37 dB.

7.0 PEDESTAL REMOVAL

The typical video output of the detector array of a TIC is characterized by the presence of a pedestal as illustrated in Figure 2. When the input RF signals are identical, a correlation peak appears on the pedestal. In order to confirm the presence of a correlation peak by a simple thresholding operation, it is convenient to remove the pedestal.

Pedestal removal techniques are based on digital post-processing of the correlograms collected by the detector array. Three possible methods have been compared at DREO [10], namely the phase shift pedestal, the average pedestal and the generated pedestal removal technique. All three methods have in common that a subtraction is made between correlograms that were formed at different times, by different segments of the input data. A brief summary and a comparison of the three techniques follows.

7.1 Phase Shift Pedestal Removal

A pedestal removal method using phase shifts has been described in the literature [19]. It relies on the subtraction of a correlogram from the previous one after a polarity change of the correlation peak produced by a 180° phase shift of the RF signal applied to one of the Bragg cells. The phase of the other signal is not changed. Figure 9a and Figure 9b illustrate the correlation peak and part of the correlogram before and after the 180° phase shift respectively. The subtraction of the signals of

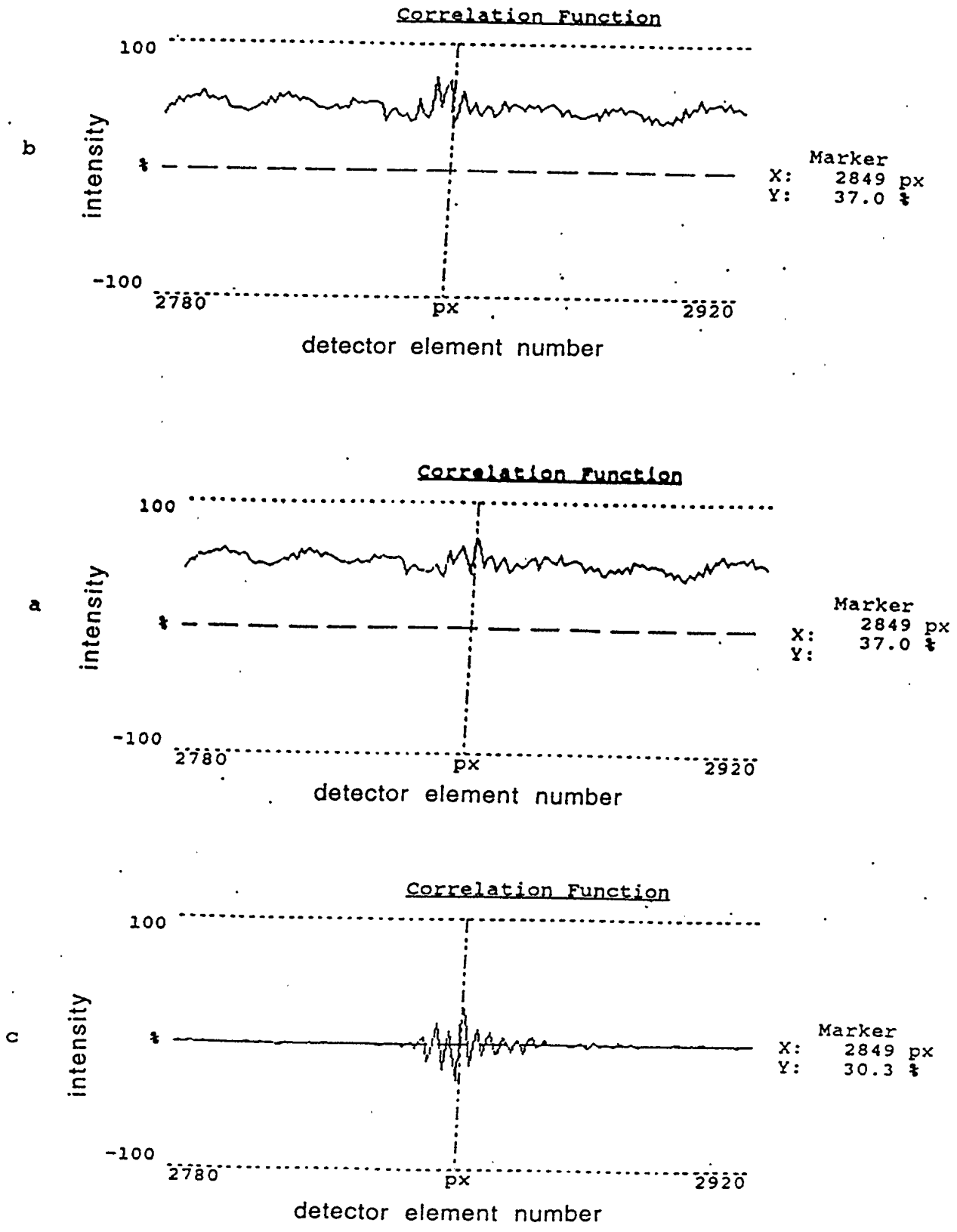

FIGURE 9: PHASE SHIFT PEDESTAL REMOVAL.

Figure 9a and 9b removes the pedestal and doubles the height of the peak as can be seen in Figure 9c.

In order to ensure complete pedestal removal and maximum enhancement of the height of the peak, it is important to have the Bragg cell filled with signal before starting the integration with the detector array. This allows the accumulation of energy in the peak to start at the beginning of the integration time, whatever the location of the peak in the time-window of the TIC.

In a typical situation, where the Bragg cells contain 50 μs of RF signal, a waiting period of 50 μs after a phase shift is required to fill the Bragg cells before starting the integration. If the integration time is 250 μs, two 50 μs delays are required while waiting for new signals to propagate through the Bragg cells. Hence it takes 600 μs to obtain a useful integration time of 500 μs. The shorter the integration time, the more significant is the loss associated with the filling time of the Bragg cells. A substantial improvement in the processing speed is possible if the pedestal removal is performed without interrupting the flow of data with phase shifts that are followed by waiting periods.

The phase shift pedestal removal technique has another feature that reduces the processing speed when short integration times are required. The detector array read-out circuitry has a minimum integration time T_{min}. In the phase shift pedestal removal method, the correlation peak is built up from two integration periods of T_{int} with a phase shift of 180° in between. The resulting minimum integration time for the phase shift pedestal removal technique is thus $2T_{min}$. This can lead to a substantial reduction of the processing speed when integration times less then $2T_{min}$ are required.

7.2 Averaged Pedestal Removal

The second pedestal removal method was proposed at DREO. It consists of subtracting from the most recent correlogram the weighted average of a few previous correlograms that did not contain a correlation peak. The averaged pedestal reference is built by adding a certain percentage of each new correlogram that does not contain peak. The process of building the reference pedestal can be described by the following equations:

$$P_i = X P_{i-1} + Y C_i$$

where

P_i = i^{th} reference pedestal,
C_i = i^{th} peakless correlogram
x,y = weighting factors such that X+Y = 1.

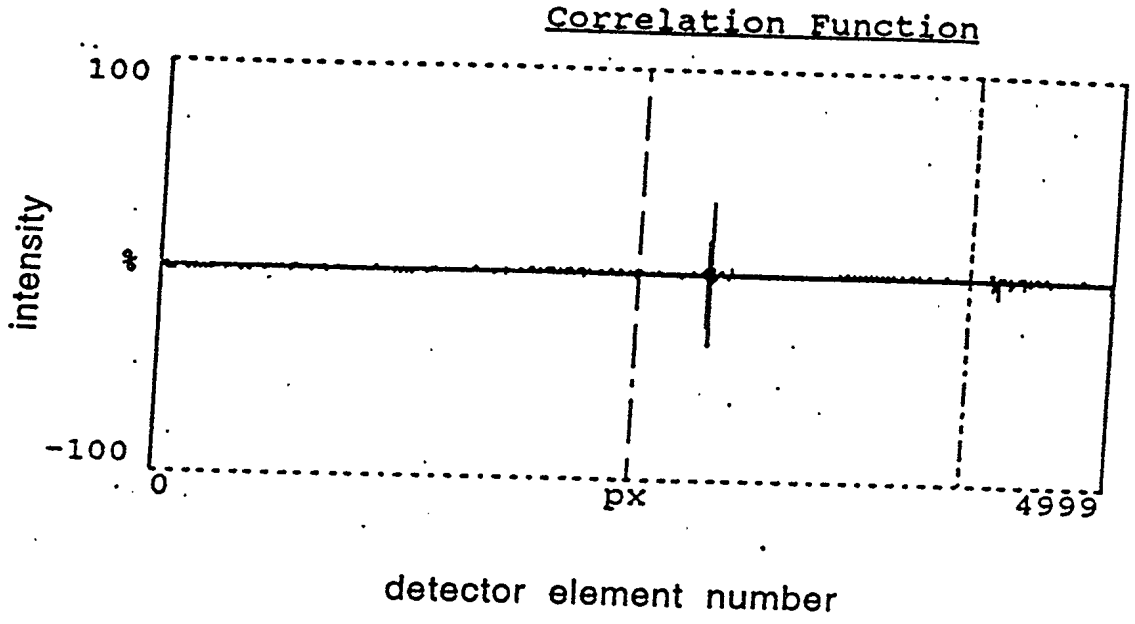

FIGURE 10: AVERAGED PEDESTAL REMOVAL.

This method leads to substantial time savings in the operation of the TIC because it is unnecessary to wait for the Bragg cells to fill up because the flow of data is not interrupted by phase shifts. Also, because the production of a peak with a averaged pedestal removal technique involves the collection of a single correlogram, the minimum integration time associated with this technique is T_{min}, the minimum integration time of the detector array. Results from this technique are illustrated in Figure 10.

7.3 Generated Pedestal Removal

A third pedestal removal method was proposed and studied at DREO. It consists of subtracting from the last collected correlogram, a stored reference correlogram that does not contain a correlation peak. The pedestal is thus removed and the peak is left intact (Figure 11). The reference is updated after a set time. Similarly to the averaged pedestal removal method, this method does not involve any waiting time for the RF signal to fill the Bragg cell because the signal is not interrupted by phase shifts. The speed of the TIC is the same as for the averaged pedestal method and the minimum integration time is also T_{min}.

7.4 Comparison of the Three Techniques

Theoretically, all three methods produce a peak with the same signal to noise ratio (S/N). When the total integration time involved in the pedestal removal process is the same, the height of the correlation peaks is the same.

In the phase shift method, the integration time is built up from two integration periods of duration T_{int} with a phase shift of 180° in between. As it is necessary to wait for the signals to propagate through the Bragg cells after every phase shift, the duration of one cycle of operation is $2T_{int}+2\tau$, where τ is the propagation time in the Bragg cell.

In the average generated pedestal methods, a single correlogram is subtracted from a stored pedestal and no waiting time is required. Thus, the cycle duration is T_{int}. If the minimum integration time of the detector array is T_{min}, the minimum integration times produced by the phase shift, the generated and the averaged pedestal removal technique are respectively, $2T_{min}$, T_{min} and T_{min}. Thus the generated and averaged pedestal removal techniques have the advantage to give access to shorter integration time than the phase shift pedestal removal technique.

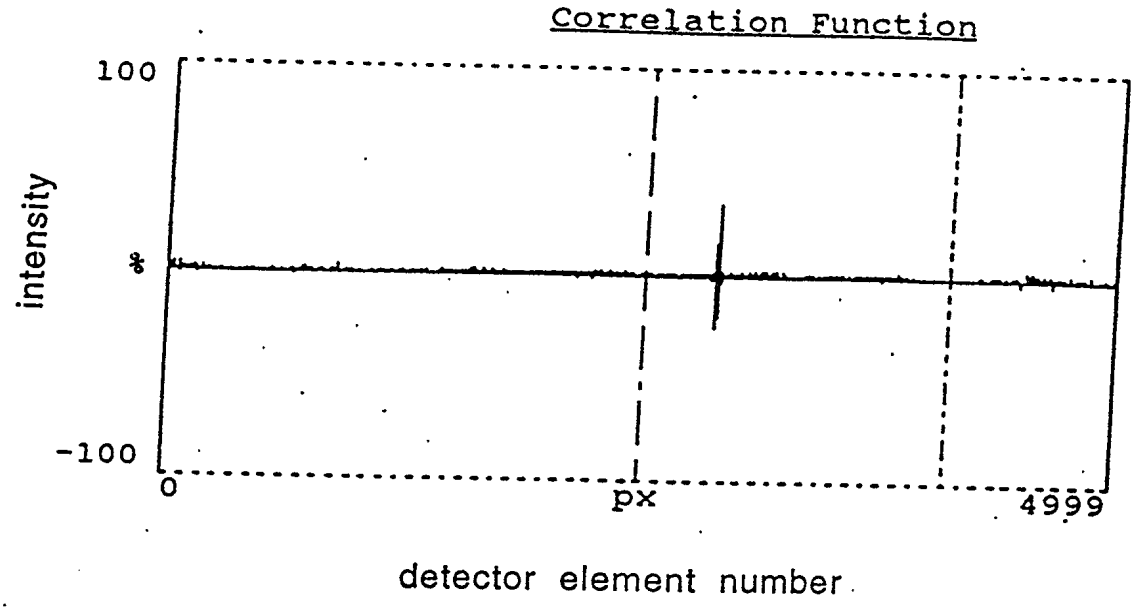

FIGURE 11: GENERATED PEDESTAL REMOVAL.

8.0 DATA COLLECTION

The study of the data collection process of a TIC is particularly interesting because of the many different output configurations possible. Some configurations have a potential for large amplitude peaks if all parameters are precisely optimized. However, small drifts in the values of the parameters can lead to low amplitude peaks that are very difficult to detect. Fortunately, it is possible to find configurations where the degradation associated with small drifts in the parameters of operation is acceptable. These results were obtained from a computer simulation of the detection process of a TIC and are fully documented in [12].

8.1 Detection Process

Let us first consider the origin of and the factors affecting the shape of the triangular envelope. The input is assumed to be a binary phase-shift keyed (BPSK) signal. The first element affecting the shape of the output signal is the triangular envelope formed by the autocorrelation of the rectangular chips modulating the sequence. The width at the base is equal to the length of the bit and is therefore equal to the velocity v of the acoustic signal in the Bragg cell divided by the bit duration. The apex of the triangular envelope is located at the meeting point of the two input signals as they propagate in the Bragg cells and it can be found anywhere within the time window of the TIC according to the difference of time of arrival of the signals.

The second element contributing to the TIC output is the modulation. In the absence of aberration or misalignment of the optical system, the period of the modulation is inversely proportional to the angle between the two beams diffracted by the Bragg cells. The modulation period can vary from infinity, when the two beams are colinear, to a very small value when the angle between the two beams is large. The period and the phase of the modulation can also be locally affected by the presence of optical aberrations or misalignments of the optical system. The phase of the modulation also depends on the phase difference of the signals applied to the Bragg cells.

The third factor contributing to the output of a TIC is the bias that is added to the product of the fringe pattern with the triangular envelope. This simulates the pedestal on which the peak appears.

8.2 Computer Simulation

A computer simulation was developed to study the amplitude of the correlation peak as a function of the various parameters of the output of a TIC. The light distribution produced by the TIC can be described by using the three following elements (Figure 12):

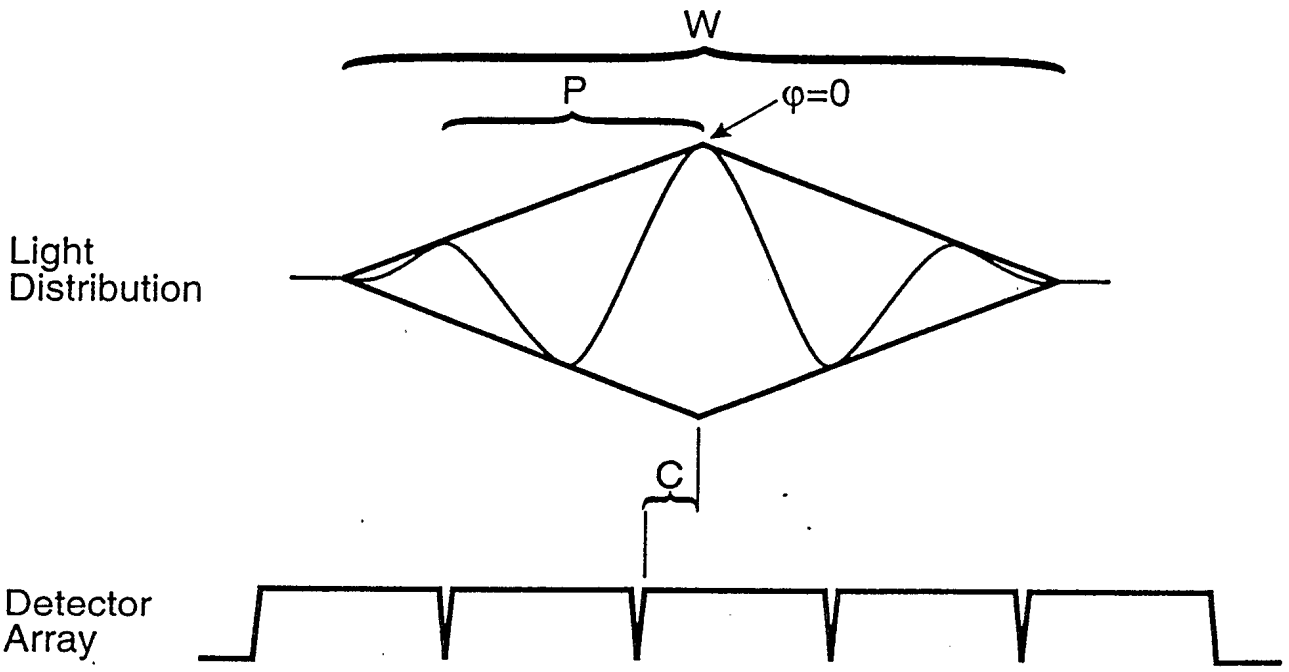

FIGURE 12: DEFINITION OF THE INPUT PARAMETERS FOR THE COMPUTER SIMULATION

1) a triangular envelope of variable width W and location C
2) a modulation of the triangular envelope with a period P,
3) a uniform bias.

All the parameters are defined in unit of number of pixels where a pixel is one element of the detector array. They are illustrated in Figure 12. The parameters are W, the width of the triangular envelope at the base, P, the period of the modulation, φ, the phase of the modulation at the apex of the triangular envelope and C, the location of the detecting elements relative to the apex of the triangular envelope.

The simulation is based on an idealized description of the factors contributing to the detection process. The detection process is modelled by a spatial integration of the energy incident on each element of the detector where the incident energy is weighted with the sensitivity response of the detecting elements. The simulation also includes the capability to use different sensitivity profiles for the detecting elements. The physical size of the detecting elements and their sensitivity profile (that may include a dead-space) and the location of the detecting elements of the array relative to the features of the light distribution are also key factors. The impact of these parameters on the detection of a correlation peak have been studied [12] for the case of no modulation and for perfect adjustment of the relative phase of the input signals.

8.3 Optimal Detection Parameters

A thorough study of the detection process, including the effect of the modulation period, of the detector sensitive profile position and of the adjustment of the relative phase of the input signals was performed at DREO and was presented in [12]. The next sections contain a brief summary of the results of this work.

8.3.1 Blind Spots

Blind spots are areas of the TIC time window where the amplitude of the peaks is too small to be detected. They occur under certain combination of the parameters of the detection process. The main object of the study presented in [12] was to determine the conditions of operation that produce blind spots and to find conditions of operation where they do not occur.

Ideally, the output of a TIC should be free of optical phase error and the phase difference of the input signals should be adjusted to produce a maximum amplitude. In this case, there is no modulation of the peak. However, these conditions are quite difficult to achieve and maintain. It requires the utilization of diffraction limited optical components, the capability to achieve and maintain near perfect alignment of the whole optical system and the precise adjustment of the phase difference of the signals applied to the Bragg cells. It has also been demonstrated [12]

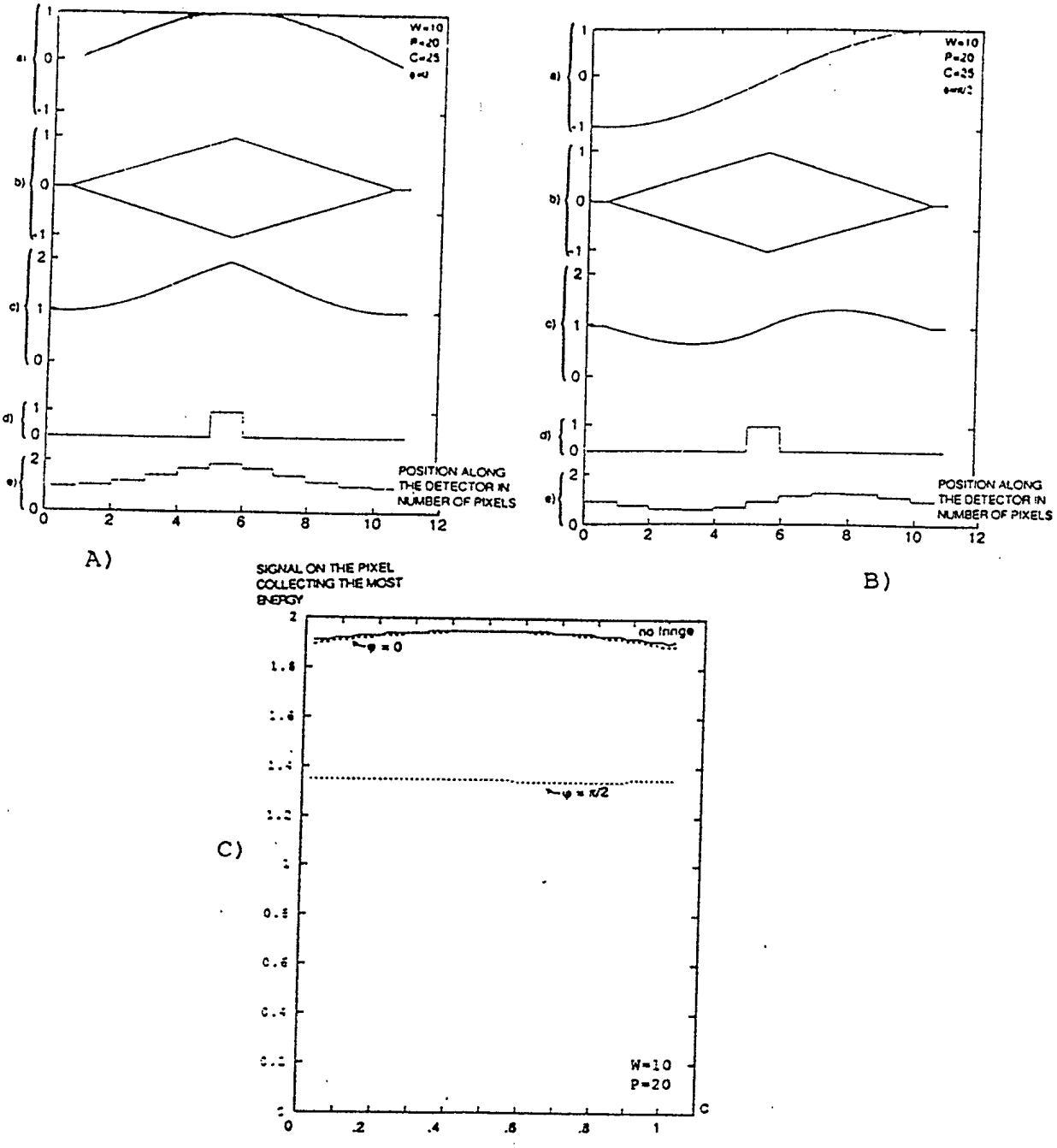

FIGURE 13: ILLUSTRATION OF THE PRODUCTION OF A BLIND SPOT. OUTPUT FROM A TIME-INTEGRATING CORRELATOR FOR A RECTANGULAR SENSITIVITY RESPONSE OF THE DETECTOR AND WITH
A) W=10, C=25, P=20 AND $\varphi=0$.
B) W=10, C=25, P=20 AND $\varphi=\pi/2$.
C) AMPLITUDE OF THE PEAK AS A FUNCTION OF THE POSITION OF THE APEX OF THE TRIANGULAR ENVELOPE ON THE DETECTING ELEMENT

that the changes of acoustic velocity in the Bragg cells associated with a temperature change as small as .09°C can cause the formation of a modulation.

Let us assume that a modulation is produced by any or a combination of the factors mentioned in the previous paragraph: a blind spot may then appear. The situation is illustrated in Figure 13 where two extreme results of the detection process are illustrated. Figure 13a corresponds to a combination of parameters with $\varphi=0$ that leads to the detection of a peak that has a large amplitude of 1.95. Figure 13b differs only by the location of the apex of the triangular envelope relative to the fringe pattern. The amplitude of the peak as a function of the position of the apex of the triangular envelope relative to the detecting element is illustrated in Figure 13c. The energy in the peak is about 1.35 for the worst case, $\varphi=\pi/2$, and the amplitude of the peak produced is, at best, difficult to detect and a blind spot in the field of view of the correlator is generated. It is obviously an unacceptable feature for a system that is expected to produce reliable peak detection.

8.3.2 Simulation Results

Further studies of the detection process with the simulation have established that it is possible to reach a compromise where stable performance of a fair quality is traded off against unpredictable performances that are either excellent or very poor. Stability in the detection process is achieved by purposefully producing at the output of the TIC a fringe pattern whose period is calculated to produce peaks with an acceptable amplitude variation for all positions of the detecting elements relative to the fringe system and the triangular envelope. A large range of values for the width W of the triangular envelope and for the period P of the fringes was systematically explored. This approach allowed to locate combination of parameters producing correlation peaks whose amplitude was sufficiently high and sufficiently constant for all positions of the peak across the detecting elements.

Figures 14, 15 and 16 present the amplitude of the peak as a function of the position of the apex of the triangular envelope on the detecting element for the combinations of parameters W and P giving the best results. In all cases the calculations have been made for the values $\varphi=0$ and $\varphi=\pi/2$ of the fringe system at the apex of the triangular envelope that correspond respectively to the highest and lowest peak amplitude. The case of a uniform background with no modulation and a perfect adjustment of the relative phase of the two input signal is added for comparison purposes because it produces the highest peak but is very sensitive to variations of the relative phase of the input signal.

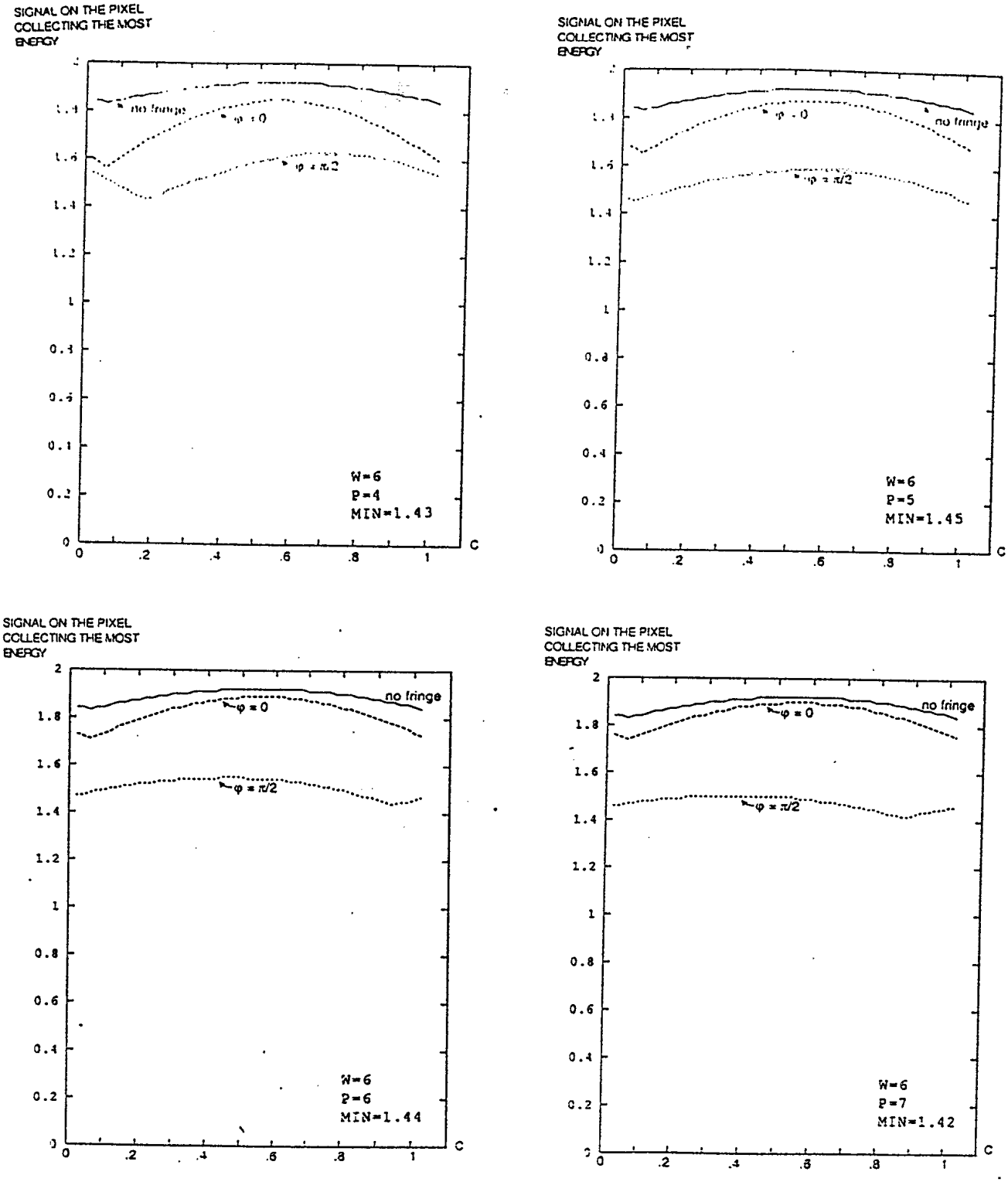

FIGURE 14: AMPLITUDE OF THE PEAK AS A FUNCTION OF THE POSITION OF THE APEX OF THE TRIANGULAR ENVELOPE ON THE DETECTING ELEMENT FOR W=6 AND P=4, 5, 6 AND 7 FOR A RECTANGULAR SENSITIVITY RESPONSE

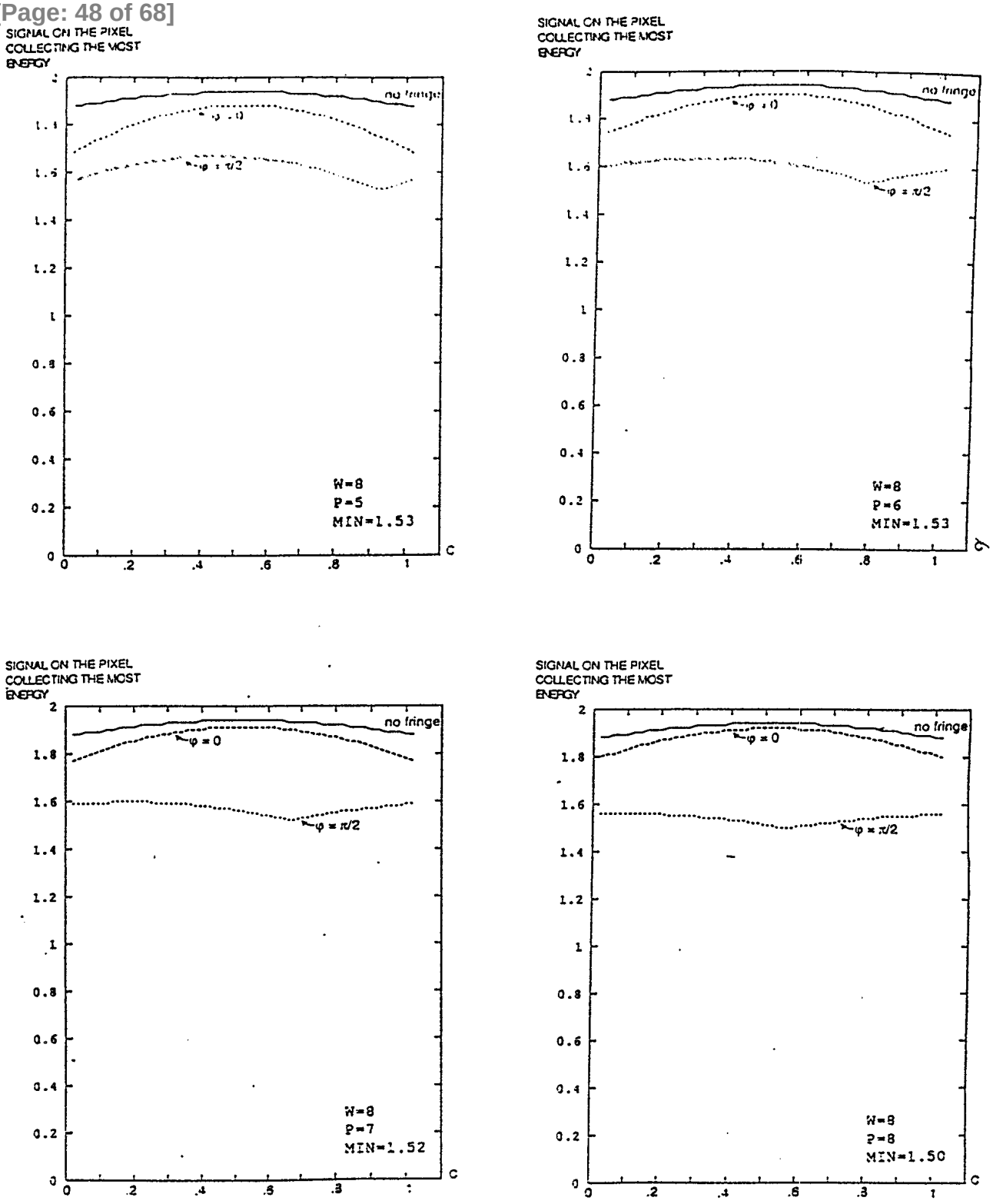

FIGURE 15: AMPLITUDE OF THE PEAK AS A FUNCTION OF THE POSITION OF THE APEX OF THE TRIANGULAR ENVELOPE ON THE DETECTING ELEMENT FOR W=8 AND P=5, 6, 7 AND 8 FOR A RECTANGULAR SENSITIVITY RESPONSE

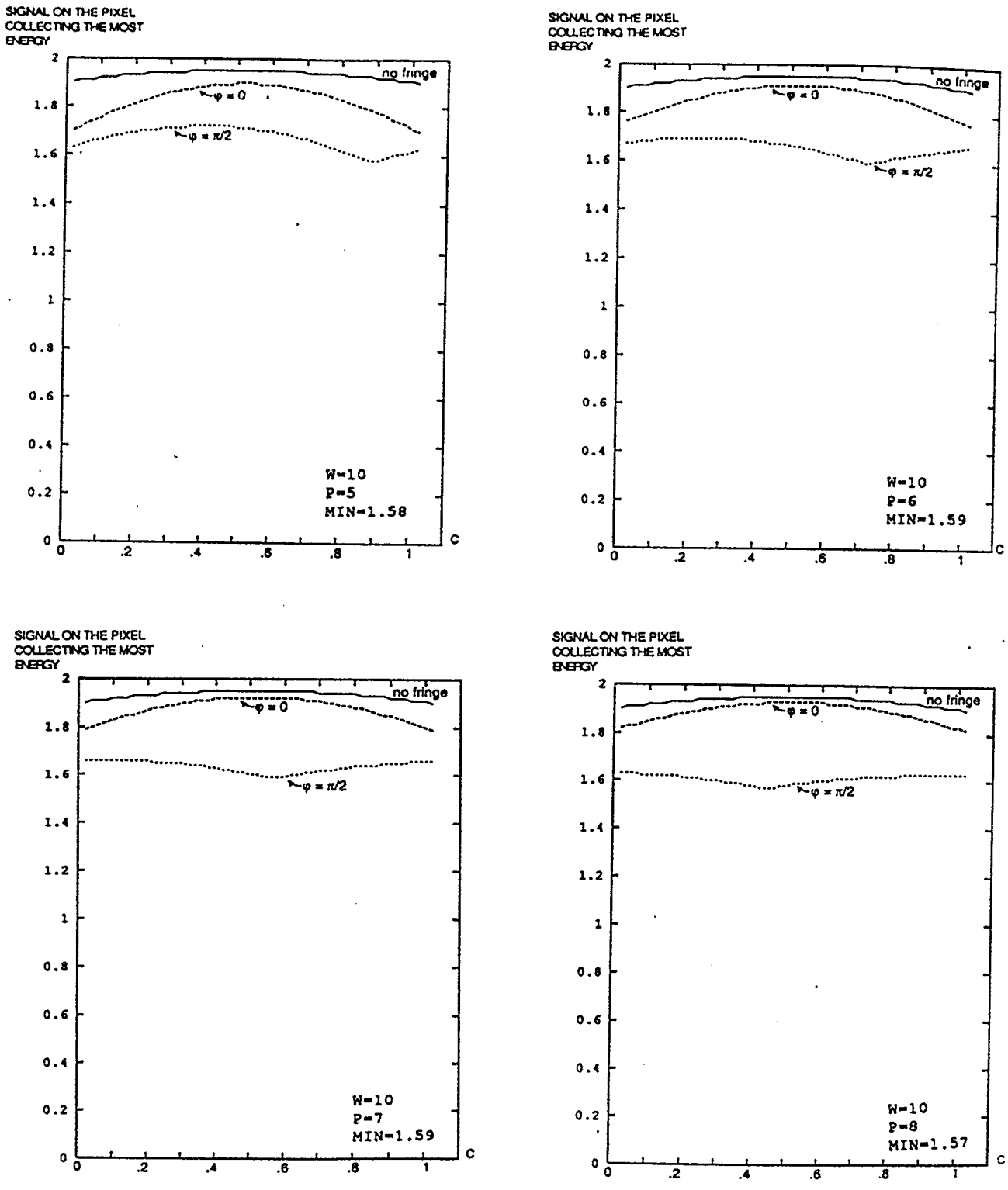

Figure 16 Amplitude of the peak as a function of the position of the apex of the triangular envelope on the detecting element for W=10 and p=5, 6, 7 and 8 for a rectangular sensitivity response.

A trend towards higher peak amplitude with increasing values of the width W of the triangular envelope is observed from the results illustrated in Figures 14, 15 and 16. A trend towards better peak amplitude uniformity with increasing fringe period P can also be observed. However, one has to remember that the width W of the triangular envelope is inversely proportional to the chip rate of the data being processed by the correlator, so large values of W leads to small values of chip rate and thus to a severe limitation of the processing speed of the correlator. A compromise has to be reached between the processing speed of the correlator and the amplitude and amplitude uniformity of the peak. The particular choice of W will depend on the speed and peak detection requirements of the system considered. Once an appropriate value for W is selected, the best value of the fringe period P should be chosen accordingly.

One particularly important feature of the detection process illustrated in Figures 14 to 16 is the graceful deterioration of the amplitude of the peak when the parameters W and P drift from their optimal values. The parameter that is the most likely to drift from its set value is the modulation period P. This is so because the presence of phase error produced by aberration, temperature change [11] or misalignment of the optical components of the system cause alteration of the fringe period of the output. The graceful deterioration is illustrated by the following example. For W=10 (see Figure 16), the amplitude of the correlation peak is 1.59 for a fringe period of six or seven pixels. However, if the value of P was to become 5 or 8, the minimum peak amplitude would be 1.58 and 1.57 respectively. It was also demonstrated [11] that the amplitude of the peak produced by the detection of an optimal modulation is very resistant to temperature change. This is in strong contrast with the case where there is no modulation and where the amplitude of the peak is very sensitive to temperature change [11].

It was also demonstrated [12] that the exact shape of the sensitivity response of the element of the detector array is a parameter of secondary importance in the evaluation of the performance of the detection process.

8.4 Experimental Verification

Experimental verifications of the performances of the detection process described in the previous sections were performed with the correlator illustrated in Figure 1. An autocorrelation of a 7-chip long pseudo random sequence was performed. The chip rate was 10 MHz and a multitude of correlation peaks appeared in the window (Figure 17). Once again, variations of the amplitude of the peaks is observed, but all peaks are detectable, and no blind spot appears.

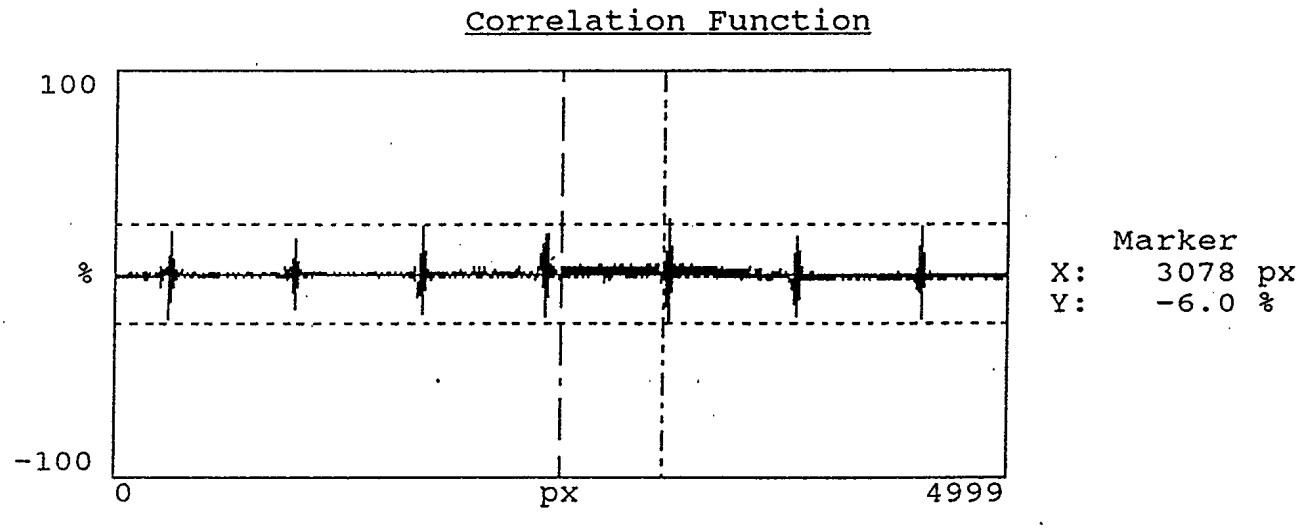

FIGURE 17: DEMONSTRATION OF PEAK DETECTION ACROSS THE TIME-WINDOW.

9.0 EFFECTS OF TEMPERATURE CHANGES ON THE OUTPUT

It has been demonstrated [20] that acousto-optic spectrum analyzers are sensitive to temperature changes and require strict temperature control to maintain the registration stability of their output. These results suggest that the effect of temperature changes on more complex interferometric systems such as TICs using two Bragg cells could be significant and an investigation was performed at DREO [11]. This section summarizes an analysis of the effects of temperature changes on the output correlation peak of a TIC presented in [11].

It is indeed possible to demonstrate that temperature fluctuations cause changes of acoustic velocity in Bragg cells and important alterations of the format of the output result. The specific effect considered is peak amplitude changes resulting from alterations of the output format. Peak positioning errors in the measurement of the time difference of arrival of the RF input signals have also been analysed and found negligible, so they will not be reviewed here.

In ideal condition, the output of a TIC is a modulated triangular envelope. If the temperature fluctuates, the acoustic velocity within the Bragg cell crystal changes thus modifying the diffraction angles of the two wavefronts and the period of the modulation.

It was demonstrated using the computer simulation described in [12] that with the width W of the triangular envelope varying between

$$8 < W < 12$$

and the period P of the modulation varying between

$$5 < P < 8,$$

the minimum amplitude of the detected peak varies between 1.50 and 1.54 for all positions C of the array of detectors relative to the location of the modulation pattern produced by the TIC (Figure 12). A minimum detectability of the correlation peak is thus ensured.

In order to assess the temperature sensitivity of the multi-fringe detection process, we calculated the temperature change required to transform a fringe pattern with a five pixel period into a fringe pattern with a six pixel period. A pixel size of 7 μm is used. It corresponds to the size of the detecting element of the Kodak array used for the construction of the TIC.

It can be calculated that an angle difference of .00163 rad. changes the fringe period from five to six pixels. The acoustic velocity change associated with that angle change is 43.58m/s. Therefore, given a temperature coefficient of the acoustic velocity of 180.6 ppm/°C, a temperature change of 387°C is necessary to increase the period from five pixels to six pixels.

As the temperature changes expected in a laboratory environment are, at the most of 20°C, this indicate that the detection of an optimally modulated peak is not sensitive to changes in temperature.

10.0 PACKAGING

One of the most important goals in the development of a prototype such as the TIC is the demonstration of reliable operation for extended period of time in a working environment. The successful integration of the TIC to the Digital Controller (DC) is also a key issue.

Reliable operation of the TIC was made possible by the careful packaging of the system using the machine shop resources available at DREO. First, the final configuration with all its components was selected, demonstrated and tested on an optical bench. This bench system was then packaged into the rack mountable 19-inch drawer illustrated in Figure 3. The packaging included an aluminium base supported by shock absorbers installed on an aluminium plate. This was necessary to isolate the TIC from the vibrations generated by the other equipment in the rack. The laser and its power supply were installed in a small compartment on the side of the drawer. Air cooling was not required. The other optical components were mounted in the larger compartment and held rigidly. Most of the holders were custom designed for this application. The drawer was installed in a rack and the performance of the TIC were tested in a laboratory environment. The results were essentially the same as the results from the bench version.

A panel installed on the back of the drawer allows the input data to reach the Bragg cells, to send control signals to the detector array and to read-out the detector array. Special attention was taken to ensure proper ground and to avoid feed through of the signals.

11.0 DIGITAL CONTROLLER

The operation of the TIC is controlled by a Digital Controller (DC). The DC controls the flow of signals to and from the TIC and the associated hardware and software. The DC provides the operator interface and allows parameters of operation to be defined. The DC also contains the algorithms used for statistical analysis of the results from the TIC. The DC is designed as a research tool and is characterized by flexibility that is achieved by software rather than hardware implement operation (two detector array read-outs per second). However, this is an acceptable feature for a research prototype whose main function is to test the processing algorithms and the performance of the TIC.

11.1 System Configuration

The system runs in the Microsoft Windows 2.1 operating environment under MS-DOS operating system on a 486 computer [21]. Windows provides a graphic interface under which several tasks can run concurrently. Standard mouse, keyboard screen and printer interfaces are provided. The DC consists of several independent tasks that run concurrently and communicate using the dynamic data exchange protocol and a few special messages. The system is implemented in the C computer language, and includes some Assembler routines where necessary. The Microsoft C 5.1 compiler and Microsoft Macro Assembler 5.1 were used. An IEEE-488 Controller is the parallel interface between the computer and the other components of the system. The DC hardware processes the output of the TIC without the intervention from the host processor. This includes pedestal removal and the detection of correlation peak above a specified threshold. The operator can select to declare the detection of a correlation peak as soon as the threshold has been met M times out of N trials. It is also possible to add many TIC outputs, each of them collected with an integration time T, to increase the effective integration time. The host processor programs the hardware when new sequences of bits are sent to the TIC from the pattern generator.

11.2 Signal Processing Algorithms

The DC contains two types of signal processing algorithms. The first type has already been described in Section 7.0 and consists of pedestal removal algorithms. The other algorithms are designed to calculate statistics on the output of the TICs and are briefly described in the following section.

Three different programs have been included in the DC for statistical analysis. The first program, Statistical Analysis [22], allows the operator to request the calculation of the mean, the variance and the standard deviation of the amplitude on two segments of a correlogram specified by the operator.

With the second program, Detection Statistics [22], repetitive tests can be defined and statistics on the detection of a correlation peak and on the position and height of the peak can be calculated. Probabilities of detection and false alarm are also calculated.

The third program, Correlogram Probability Distribution [22] is used to calculate probability distributions from the histogram of the absolute value of the amplitude and selected pixels. The probability-density function or the cumulative-distribution function can then be calculated.

12.0 EXPERIMENTAL RESULTS

The performances of the system described in the previous sections were evaluated by a series of experimental measurements and the results were compared, when possible, to theoretically achievable results. The TIC has a bandwidth of 30 MHz and BPSK signals with a chip rate of up to 20 MHz were used for testing. The capability of the TIC to produce correlation peaks of uniform height, without blind spots, over the whole time-window was demonstrated. The capability of the TIC to detect small signals was also tested experimentally and the dynamic range of the TIC was found to be 50 dB. Finally the capability of the TIC to extract correlation peaks from noisy signals was tested and it was found that detectable peaks were produced with a SNR of -35 dB with a processing gain of 40 dB. The TIC was thus performing very close to the theoretical limit.

12.1 Test Signals and Processing Gain

It was decided to test the system using BPSK signals generated with maximal-length direct sequences as spreading codes. These signals are wideband signals which produce a nearly ideal triangular auto-correlation peak of known width (Figure 18). Chip rate of up to 20 MHz were used.

In order to be able to compare the actual performances of the TIC against a theoretical benchmark it is necessary to introduce the concept of processing gain as it applies to the processing of noisy direct-sequence spread spectrum signals. The despreading of a spread spectrum sequence is performed by a correlation of the noisy signal with a clean replica of itself. The processing gain is then defined as the number of integrated chips and is equal to the product of the chip rate used to spread the sequence by the integration time. For example, an integration time of 1 ms with a chip rate of 10 MHz gives a processing gain of 10,000 or 40 dB. In that case, if the signal being despread had a SNR of -30 dB, the correlation peak would have a SNR of 10 dB if it was produced by a perfect correlator. It is the yardstick that will be used here to assess the performances of the TIC developed at DREO. Any further reduction in the SNR of the peak is attributed to correlation losses caused by an imperfect correlator.

12.2 Uniformity Across the Time-Window

One of the most desirable features of a TIC is the production of correlation peaks of uniform height over the whole time-window of operation. This capability depends on the successful production of a uniform pedestal and on the elimination of blind spots by using an appropriate data collection technique. The TIC developed at DREO was tested by auto correlating a short direct sequence at a chip rate of 10 MHz. Multiple correlation peaks are produced at every repeat of the sequence. If the TIC illumination was perfectly uniform, the only fluctuation in peak

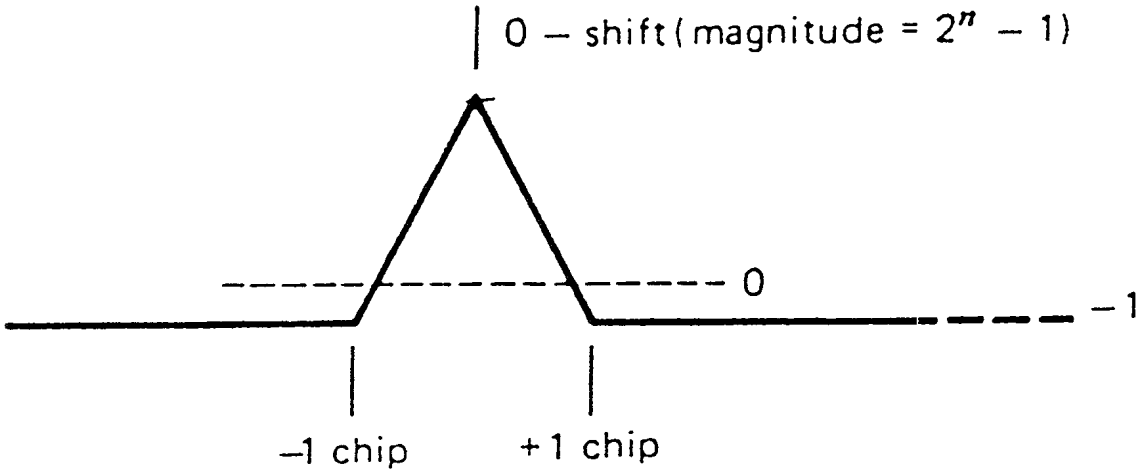

FIGURE 18: FULL PERIOD AUTOCORRELATION OF A MAXIMUM LENGTH DIRECT SEQUENCE.

amplitude would be caused by the location of the element of the detector array relative to the features of the peaks. A typical result for a 32-chip long sequence and a 10 MHz chip rate is illustrated in Figure 19.

12.3 Weak Signal Detection

Another important aspect of the performance of a TIC is its capability to detect weak signals. The ratio of the strongest detectable signal to the weakest detectable signal is called dynamic range and is usually expressed in dB. The dynamic range of the TIC was measured by applying to one Bragg cell a direct sequence with a power of 1W. The same sequence, at reduced level was applied to the other Bragg cell. Figure 20 illustrate the correlation produced when the weak signal is at 55 dB and 60 dB below the strong one. An integration time of 2 ms and a chip rate of 20 MHz were used. An easily detectable correlation peak is produced in both cases.

12.4 Detection of Signals in Noise

A particularly remarkable feature of TICs is the ability to detect the presence of signals having a very low SNR. The confirmation of this capability was obtained by applying to one of the Bragg cells a direct sequence with a power of .5w. Figure 21 illustrates the correlation peaks obtained with SNRs of -30 dB, -32 dB and -35 dB. The integration time was 1 ms, the chip rate was 10 MHz and the resulting processing gain was 40 dB. Figure 21 clearly demonstrates the capabilities of the TIC to produce processing gains that come very close to the theoretical limit and compare well to the correlation losses of 2-3 dB that are typical of digital correlators [23].

13.0 CONCLUSION

This report describes the design and performance of a TIC built at DREO for the processing of spread spectrum signals. A general description of the TIC, of its operation, components and subsystems is presented. The signal processing and the data collection procedure are also described. The digital controller, the packaging of the system and the effects of the temperature changes on the stability of the TIC are presented. The TIC has a 30 MHz bandwidth and BPSK signals with chip rate of up to 20 MHz were used to test the system. Experimental measurements of the performances of the TIC are included. The prototype has demonstrated the capability to detect reliably correlation peaks for a time difference of arrival window of 90 μs. The dynamic range of the TIC was measured to be 60 dB and it can produce detectable correlation peaks in additive white Gaussian noise for input signals having a signal to noise ratio of -35 dB while using a processing gain of 40 dB. The performances of the TIC is then within 5 dB from the theoretical limit.

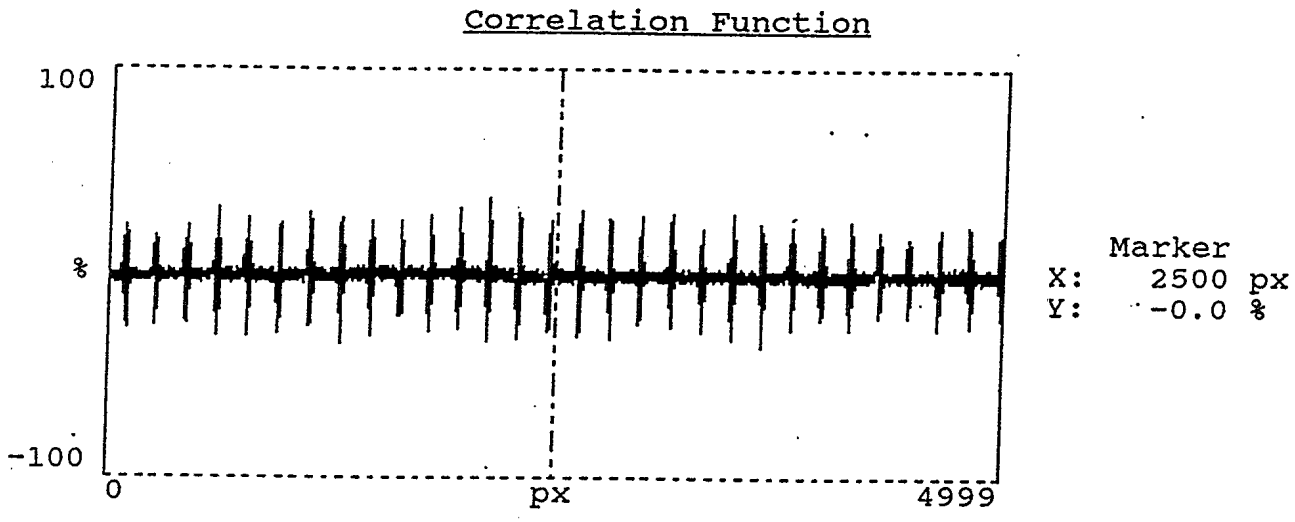

FIGURE 19: AUTOCORRELATION OF A 31-CHIP LONG MAXIMUM LENGTH SEQUENCE (NO ADDED NOISE).

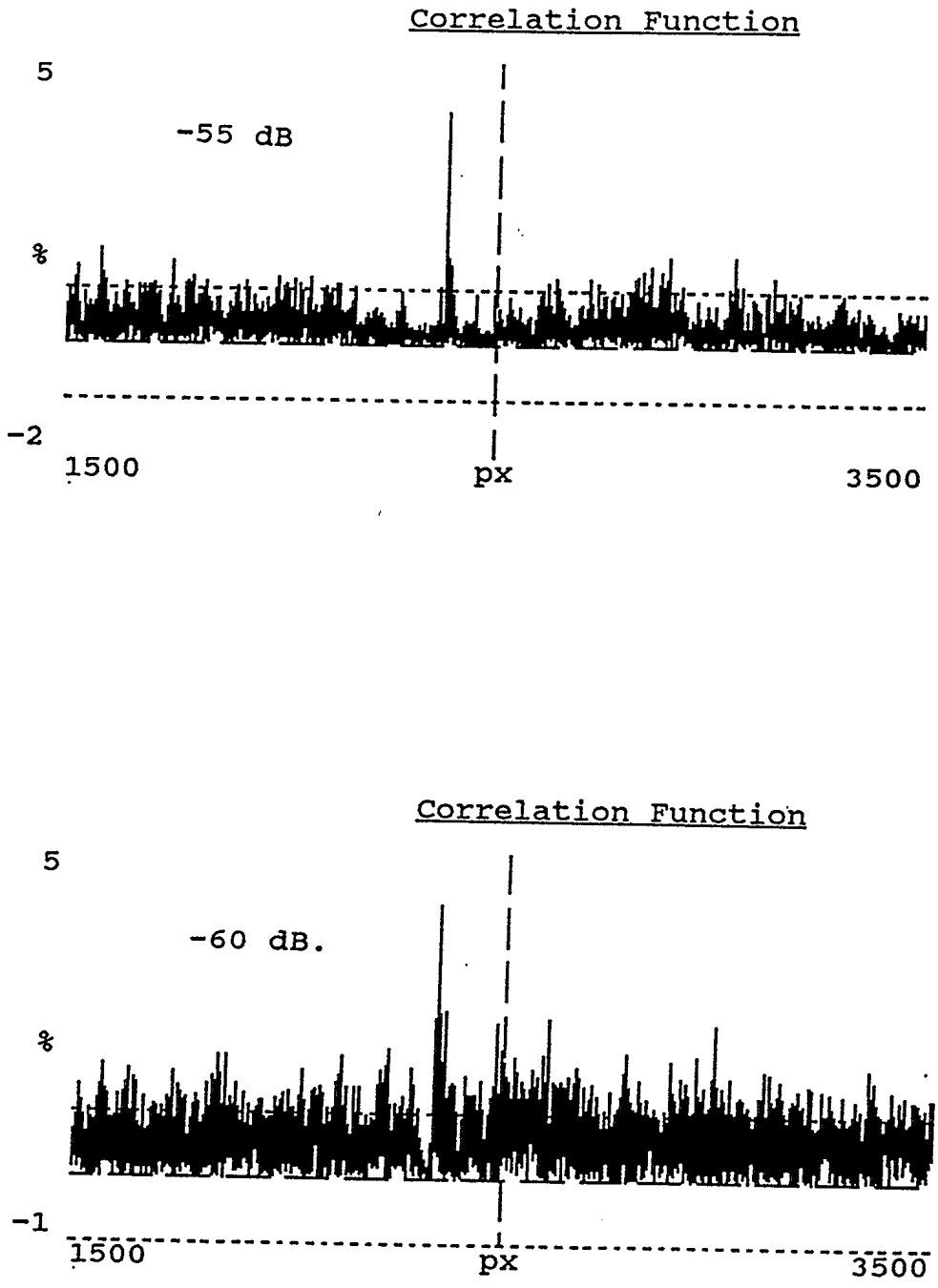

FIGURE 20: DETECTION OF SIGNALS AT -55 dB AND -60 dB.

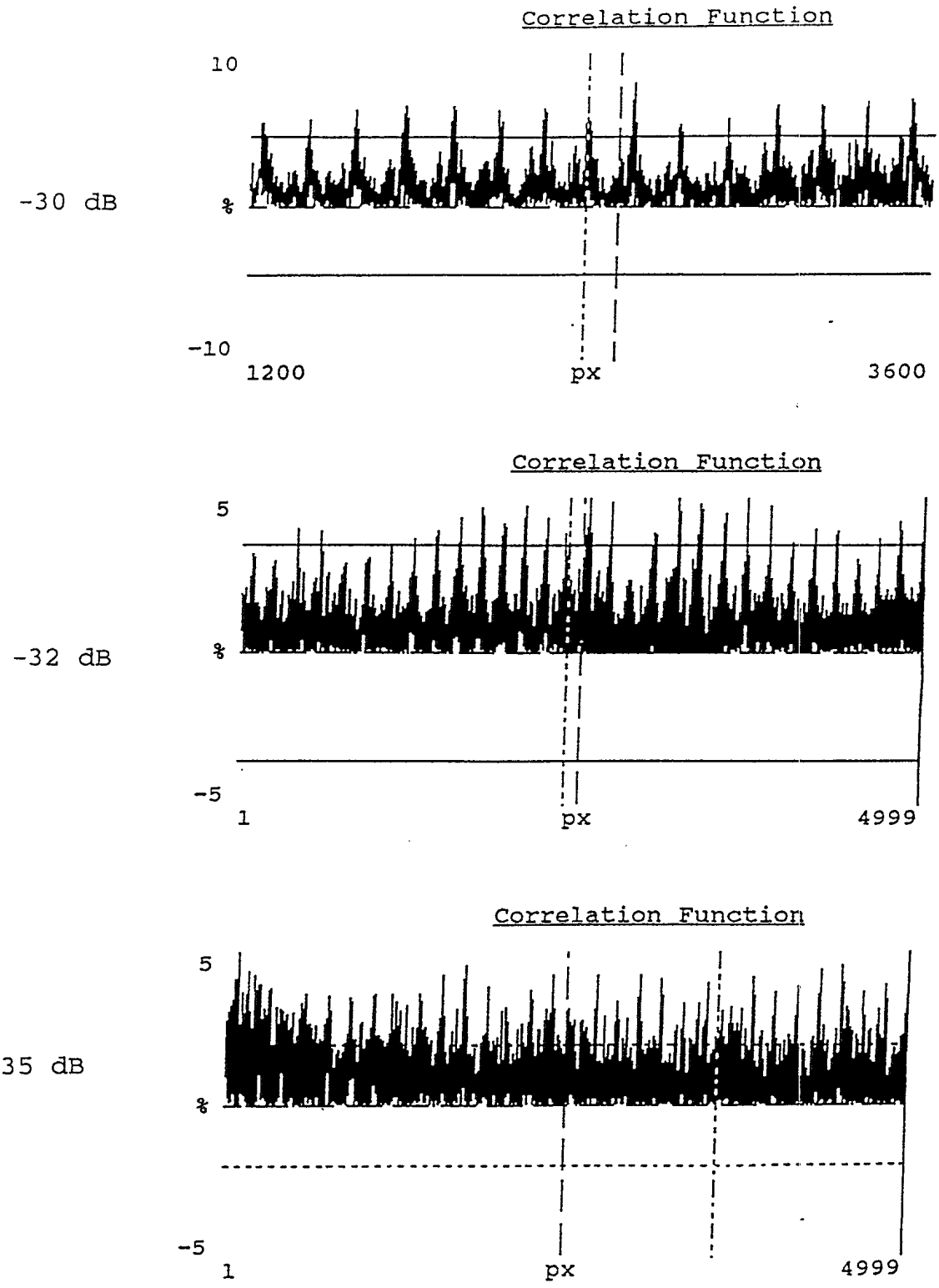

FIGURE 21: CORRELATION PEAK PRODUCED BY A CLEAN SIGNAL AND A NOISY SIGNAL WITH DIFFERENT SNR.

The TIC in its present condition, was used to perform two proof-of-concept experiments for the processing of spread spectrum signals [1,2]. In the first experiment, a TIC was used to perform signal compression of low probability of intercept radar signals using a BPSK modulation[1]. In the second experiment, a TIC was used for the real-time implementation of the cyclic crosscorrelation [2]. This algorithm has the capability to separate spread spectrum signals sharing the same bandwidth, the same carrier frequency and the same difference of time of arrival at negative signal to noise ratios. Because of these attributes, the real-time implementation of the cyclic crosscorrelation has a great potential for the development of ELINT and ESM receivers for spread spectrum signals. The further development of this potential could include the construction of a miniature version of a TIC using diode laser and packaging that would allow the system to operate in tactical military exercises.

The capability of the TIC to perform searches in large unstructured databases was demonstrated by a proof-of-concept experiment where human DNA sequences were analysed [3-4].

The optoelectronic system made of the TIC and the digital controller (DC) could be improved by an upgrade of the read-out electronic of the DC. The occasional production of a bad frame of data could be the indication of timing problems. It would also be a great improvement to fully take advantage of the processing power of the TIC by reading and processing all the data generated by the detector array. At this time only two frames per second are processed on a possible total of 5000.

14.0 REFERENCES

[1] D. Elsaesser, "A Direct Sequence Spread-Spectrum CW Radar Using an Acousto-Optic Time-integrating Correlator", DREO TN to be published.

[2] N. Brousseau and J.W.A. Salt, "Real-Time Analysis of a Spread Spectrum Environment with an Optoelectronic Cyclic Crosscorrelation: Proof of Concept Experiments", DREO TN 95-14 .

[3] N. Brousseau, R. Brousseau, J.W.A. Salt, L. Gutz and M.D.B. Tucker, "Analysis of DNA Sequences by an Optical Time-Integrating Correlator", Applied Optics, Vol. 31, No. 23, 10 Aug. 1992, p. 4802-4815.

[4] N. Brousseau, R. Brousseau, J.W.A. Salt, L. Gutz and M.D.B. Tucker, "Analysis of DNA Sequences by an Optical Time-Integrating Correlator: Proof-of-Concept Experiments", DREO TN 92-12.

[5] C.S. Anderson, A.F. Zwilling and M.C. Zari, "Wideband Acousto-Optic Processor for ESM Applications", SPIE vol. 1704, Advances in Optical Information Processing V, p. 10-18, 1992.

[6] J. Wood and M. Koontz, "Transition of Acousto-Optic into ELINT and ESM Systems", SPIE vol. 1704, Advances in Optical Information Processing V, 1992, p. 2-8.

[7] D.C. Hartup and W.T. Rhodes, "Acousto-Optic Processor for Carrier Frequency and Envelope Modulation Analysis", SPIE vol. 1704, Advances in Optical Information Processing V,1992, p. 98-104.

[8] M.C. Zari and R.J. Berinato, "Multichannel Optical Time-Integrating Correlator for Adaptive Jamming Cancellation", SPIE vol. 1704, Advances in Optical Information Processing V, 1992, p. 88-97.

[9] E.A. Viveiros, L.J. Harrison, R.J. Berinato and R.A. Durrett, "Acousto Optic Range-Doppler Processor Insertion into an Advance Spread Spectrum Radar", SPIE vol. 2236, Advances in Optical Information Processing VI, p. 39-43, 1994.

[10] N. Brousseau and J.W.A. Salt, "A Comparison of Three Pedestal Removal Techniques for an Optical Time-integrating Correlator", DREO TN 94-16.

[11] N. Brousseau, "Effects of Temperature Changes on the Output of Time-Integrating Correlators, DREO TN 93-30.

[12] N. Brousseau and J.W.A. Salt, "Analysis and Optimization of the Data Collection Process of Time-Integrating Correlators", DREO TN 95-5.

[13] I. Powell, "Design of a Laser Beam Line Expander", Applied Optics, vol. 26,1 Sept. 1987, p. 3705-3709. .

[14] "Development of a Holographic Illumination System to Update a Time-Integrating Correlator (TIC) with a 5000-Element Detector", Lasiris Inc., Final Report, contract W7714-2-9694/01-SV, Aug. 1993.

[15] S. Wofford, G. Petrie and D.L. Hecht,"Polarization Effects in Shear Wave Tellurium Dioxide Acousto-Optic Devices", SPIE vol.202, Active Optical Devices, 1979, p.180-185.

[16] M. Amano, G. Elston and J. Lucero," Materials for Large Time Aperture Bragg Cell", SPIE 567, Advances in Materials for Active Optics, 1985, p.142-149.

[17] G. Elston,"Optically and Acoustically Rotated Slow Shear Bragg Cells in TeO2", SPIE vol.936, Advances in Optical Information Processing, 1988, p.95-101.

[18] E.H. Young and H.C. Ho, "Optically Rotated Long Time Aperture TEO2 Bragg Cells", SPIE vol.1296, Information Processing IV, 1990, p.304-315.

[19] M.W. Casseday, N.J. Berg, I.J. Abramovitz and J.N. Lee, "Wide-Band Signal Processing Using Two-Beam Surface Acoustic Wave Acoustooptic Time Integrating Correlator", IEEE Transactions on Sonics and Ultrasonics, vol. SU-28, no. 3, p. 205-212, May 1981.

[20] T.E.Dimmick, P.A. Satorius and J. Fewer, Jr.,"Temperature Sensitivity of Acoustic Velocity and Frequency Registration in Acousto-Optic Spectrum Analyser", Appl. Opt. 31, 14, 10 May 1992, p. 2409-2411.

[21] M. Power, "Acousto-Optical Signal Processing Development Facility: Time-Integrating Correlator/Operator's Manual", Miller Communications Systems, DSS File No. W7714-7-5396.

[22] B. Baker, "Acousto-Optical Post-Processor Time-Integrating Correlator Updates: Final Report:, Calian Communications System Ltd., DSS File No. W7714-0-9886, March 1991.

[23] D.L. Nicholson, "Spread Spectrum Signal Design, LPE and AJ Systems", Computer Science Press, p. 134 and 196, 1988.

DOCUMENT CONTROL DATA

(Security classification of title, body of abstract and indexing annotation must be entered when the overall document is classified)

1. ORIGINATOR (the name and address of the organization preparing the document. Organizations for whom the document was prepared, e.g. Establishment sponsoring a contractor's report, or tasking agency, are entered in section 8.)

NATIONAL DEFENCE
DEFENCE RESEARCH ESTABLISHMENT OTTAWA
SHIRLEYS BAY, OTTAWA, ONTARIO K1A 0Z4 CANADA

2. SECURITY CLASSIFICATION (overall security classification of the document. including special warning terms if applicable)

UNCLASSIFIED

3. TITLE (the complete document title as indicated on the title page. Its classification should be indicated by the appropriate abbreviation (S,C or U) in parentheses after the title.)

DEVELOPMENT OF A TIME-INTEGRATING CORRELATOR FOR THE PROCESSING OF SPREAD SPECTRUM SIGNALS (U)

4. AUTHORS (Last name, first name, middle initial)

BROUSSEAU, NICOLE AND SALT, JAMES W.A.

5. DATE OF PUBLICATION (month and year of publication of document)	6a. NO. OF PAGES (total containing information. Include Annexes, Appendices, etc.)	6b. NO. OF REFS (total cited in document)
JULY 1996	56	23

7. DESCRIPTIVE NOTES (the category of the document, e.g. technical report, technical note or memorandum. If appropriate, enter the type of report, e.g. interim, progress, summary, annual or final. Give the inclusive dates when a specific reporting period is covered.)

DREO REPORT

8. SPONSORING ACTIVITY (the name of the department project office or laboratory sponsoring the research and development. Include the address.)

NATIONAL DEFENCE
DEFENCE RESEARCH ESTABLISHMENT OTTAWA
SHIRLEYS BAY, OTTAWA, ONTARIO K1A 0Z4 CANADA

9a. PROJECT OR GRANT NO. (if appropriate, the applicable research and development project or grant number under which the document was written. Please specify whether project or grant)	9b. CONTRACT NO. (if appropriate, the applicable number under which the document was written)
1410SM 5BB16	

10a. ORIGINATOR'S DOCUMENT NUMBER (the official document number by which the document is identified by the originating activity. This number must be unique to this document.)	10b. OTHER DOCUMENT NOS. (Any other numbers which may be assigned this document either by the originator or by the sponsor)
DREO REPORT 1298	

11. DOCUMENT AVAILABILITY (any limitations on further dissemination of the document, other than those imposed by security classification)

(XX) Unlimited distribution
( ) Distribution limited to defence departments and defence contractors; further distribution only as approved
( ) Distribution limited to defence departments and Canadian defence contractors; further distribution only as approved
( ) Distribution limited to government departments and agencies; further distribution only as approved
( ) Distribution limited to defence departments; further distribution only as approved
( ) Other (please specify):

12. DOCUMENT ANNOUNCEMENT (any limitation to the bibliographic announcement of this document. This will normally correspond to the Document Availabilty (11). However, where further distribution (beyond the audience specified in 11) is possible, a wider announcement audience may be selected.)

13. ABSTRACT (a brief and factual summary of the document. It may also appear elsewhere in the body of the document itself. It is highly desirable that the abstract of classified documents be unclassified. Each paragraph of the abstract shall begin with an indication of the security classification of the information in the paragraph (unless the document itself is unclassified) represented as (S), (C), or (U). It is not necessary to include here abstracts in both offical languages unless the text is bilingual).

An optoelectronic processor was built at DREO for the detection and processing, in presence of noise and interfering signals, of spread spectrum radar and communication signals . The design and performance of the processor, a Time-Integrating Correlator (TIC), are presented. A general description of the TIC, of its operation, components and subsystems is included. The signal processing and the data collection procedure are also described. The digital controller, the packaging of the system and the effects of the temperature changes on the stability of the TIC are presented.

Experimental measurements of the performance of the TIC were performed with binary phase shift keyed input signals with chip rates up to 20 MHz and the resulted are included. The TIC has a 30 Mhz bandwidth and can detect reliably correlation peaks on a time difference of arrival window of 90 μs. The dynamic range of the prototype is 60 dB and it can produce detectable correlation peaks in additive white Gaussian noise for input signals having a signal to noise ratio of -35 dB while using a processing gain of 40 dB. The performance of the TIC, for that particular set of parameters, is thus within 5 dB from the theoretical limit.

14. KEYWORDS, DESCRIPTORS or IDENTIFIERS (technically meaningful terms or short phrases that characterize a document and could be helpful in cataloguing the document, They should be selected so that no security classification is required. Identifiers, such as equipment model designation, trade name, military project code name, geographic location may also be included. If possible keywords should be selected from a published thesaurus. e.g. Thesaurus of Engineering and Scientific Terms (TEST) and that thesaurus-identified. If it is not possible to select indexing terms which are Unclassified, the classification of each should be indicated as with the title.)

TIME-INTEGRATING CORRELATOR
CORRELATION
SIGNAL PROCESSING

#500782